Contribution from the Laboratoire de Chimie de Coordination, Associé au CNRS (ERA 670), Université Louis Pasteur, 67070 Strasbourg Cédex, France, and Laboratoire de Minéralogie-Cristallographie, Associé au CNRS (ERA 162), Université de Nancy I, 54037 Nancy, France

Comparison of Two Strategies toward the Syntheses of Platinum Mixed-Metal Clusters. Reactivity of Linear M–Pt–M and Mn–Pt–Mn Complexes. X-ray Crystal Structures of $Pt_2M_2(\eta^5\text{-}C_5H_5)_2(\mu_3\text{-}CO)_2(\mu\text{-}CO)_4(PEt_3)_2$ with M = Cr, Mo, and W[1]

ROBERT BENDER,[2a] PIERRE BRAUNSTEIN,*[2a] JEAN-MARC JUD,[2a] and YVES DUSAUSOY[2b]

Received September 30, 1983

The new linear trimetallic complexes *trans*-$Pt[M(CO)_3Cp]_2(PhCN)_2$ [M = Cr (**1a**), Mo (**2a**), W (**3a**)] have been isolated and characterized. The isocyanide complexes *trans*-$Pt[Cr(CO)_3Cp]_2(t\text{-}BuNC)_2$ (**1b**) and *trans*-$Pt[Cr(CO)_3Cp]_2[c\text{-}C_6H_{11}NC]_2$ (**1c**) have also been prepared because they are related to **1a**. The first reported ν(Pt–Cr) frequencies are 173, 174, and 177 cm^{-1} for **1a–c**, respectively. The complex *trans*-$Pt[Mn(CO)_5]_2(PhCN)_2$ (**4a**) has also been synthesized. It reacts with PPh_3 to give the $Pt_5(CO)_6(PPh_3)_4$ cluster and with CO to afford the linear trimetallic *trans*-$Pt[Mn(CO)_5]_2(CO)_2$ (**4d**) complex. The syntheses, characterizations, and X-ray structures of a family of new heterotetrametallic clusters $Pt_2M_2Cp_2(CO)_6(PR_3)_2$ [Cp = η^5-C_5H_5; M = Cr (**5**), Mo (**6**), W (**7**); R = Me (**e**), Et (**f**), *n*-Bu (**g**), Ph (**h**)] are described. Two different synthetic routes have been shown to lead to these clusters. In method A, the $PtCl_2(PR_3)_2$ complexes were reacted with 2 equiv of $Na[M(CO)_3Cp]$ in THF. A complex redox reaction occurs, accompanied by ligand transfer and cluster formation. Thus, the dimers $[M(CO)_3Cp]_2$ and/or derivatives thereof such as the new $Mo_2(CO)_5(PMe_3)Cp_2$ were obtained, together with the mixed-metal clusters in which only one PR_3 ligand is coordinated to each Pt atom. Method B involves the reaction in THF of 1 equiv of phosphine with the linear trimetallic complexes **1a–3a**. Substitution of PhCN for PR_3 induces a fragmentation of the complex into reactive units that combine with each other, affording the stable compounds. Mechanisms involving radical intermediates are proposed for these reactions. In general, method B presents significant advantages over method A, namely (i) higher cluster yield (up to 87%), (ii) a readily available stable platinum precursor, and (iii) generality and economy of introduction of a phosphine ligand into a cluster molecule. An X-ray diffraction study has been performed on the complexes $Pt_2M_2Cp_2(\mu_3\text{-}CO)_2(\mu\text{-}CO)_4(PEt_3)_2$ [M = Cr (**5f**), Mo (**6f**), W (**7f**)]. Data for **5f**: monoclinic, space group $P2_1/c$ with $Z = 2$, $a = 10.765$ (6) Å, $b = 9.430$ (4) Å, $c = 17.450$ (5) Å, $\beta = 115.37$ (2)°, ρ(calcd) = 2.13 g cm^{-3}. For 2321 reflections with $I > 3\sigma(I)$, $R = 0.032$. Data for **6f**: triclinic, space group $P\bar{1}$ with $Z = 2$, $a = 10.026$ (2) Å, $b = 11.155$ (4) Å, $c = 15.126$ (4) Å, $\alpha = 85.17$ (2)°, $\beta = 75.44$ (2)°, $\gamma = 84.33$ (2)°, ρ(calcd) = 2.29 g cm^{-3}. For 4574 reflections with $I > 3\sigma(I)$, $R = 0.051$. There are two slightly different molecules, A and B, in the unit cell. Complex **7f** crystallizes in two different monoclinic cells, of $P2_1/n$ space group with $Z = 2$: $a = 8.768$ (7), 11.920 (2) Å; $b = 14.147$ (2), 12.930 (6) Å; $c = 13.580$ (6), 12.166 (3) Å; $\beta = 77.96$ (5), 61.72 (2)°; ρ(calcd) = 2.60 g cm^{-3}; 2365, 1921 reflections with $I > 3\sigma(I)$, $R = 0.033$, 0.085 for types A and B, respectively. All these structures are characterized by a planar, triangulated parallelogram framework for the metallic core. The center of symmetry of these molecules is at the middle of the Pt–Pt′ bond. This distance is rather short, ranging from 2.612 (1) (in **5f**) to 2.677 (1) Å (in **6f** A). The Pt–M distances have values of 2.748 (1) and 2.709 (1) Å for M = Cr and range from 2.777 (2) to 2.846 (1) Å for M = Mo and from 2.775 (1) to 2.836 (1) Å for M = W. A shorter Pt–M distance is found where the contributions of the bridging carbonyls on this bond is higher. In these 58-electron clusters, the 18-electron $[CpM(CO)_3]^-$ fragments bridge the L→Pt(I)–Pt(I)←L unit in a very original way: a three-legged piano-stool structure with the two Pt atoms located within the $M(CO)_3$ cone. Each PEt_3 ligand is coordinated to a Pt atom with a Pt′–Pt–P angle between 169.7 (1) and 177.7 (1)° and an average Pt–P distance of 2.285 Å. The planes of the η^5-Cp ligands are by symmetry parallel to each other and form a dihedral angle between 75.6 and 86.9° with the metallic plane. The carbonyl ligands C(1)O(1) and C(3)O(3) are semibridging the M–Pt′ and M–Pt edges, respectively, whereas C(2)O(2) is semi triply bridging the heterotrimetallic face MPtPt′. By symmetry, an identical geometry is found with the carbonyls bridging M′Pt,M′Pt′ and M′PtPt′. This bonding situation is compared in the Pt_2Cr_2, Pt_2Mo_2, and Pt_2W_2 clusters and related to the difference observed between the Pt–M and Pt′–M distances. Spectroscopic, IR, and ^1H, $^{13}C\{^1H\}$, and $^{31}P\{^1H\}$ NMR data indicate that all the Pt_2M_2 clusters presented here have the same basic structures as **5f**, **6f**, and **7f** and that the solid-state structure is retained in solution. ^1J(PtPt) values of 775 and 1039 Hz were found for **6g** and **7g**, respectively.

Introduction

Mixed-metal cluster synthesis has been recognized as a major challenge to organometallic chemists.[3] Elegant rational syntheses have only recently become available in some cases.[4,5] However, it often remains difficult or even impossible to predict the molecular formula of a cluster that could result from a given reaction. Once a reaction has been found that leads to cluster synthesis, it is of great importance to understand the influence of all parameters that govern this reaction. Among these, the natures of the transition metals and of their coordinated ligands in the precursor molecules are obviously of highest importance.

We have recently reported the syntheses and the structures of a series of tetrametallic mixed-metal clusters containing palladium and a group 6 metal M, of general formula $Pd_2M_2Cp_2(CO)_6(PR_3)_2$.[1] They are characterized by a planar centrosymmetric arrangement of the four metal atoms. In the present paper, we report on the analogous "Pt_2M_2" clusters for which the same type of tetrametallic triangulated parallelogram is found. As for the "Pd_2M_2" clusters, two different synthetic methods have led to these new Pt_2M_2 clusters. The first, method A, involves the reaction of square-planar d^8 *cis*- or *trans*-$PtCl_2L_2$ complexes (L = tertiary phosphine) with the sodium carbonylmetalates $Na[M(CO)_3Cp]$ (M = Cr, Mo, W). A preliminary note has described part of these results.[6] The second and new method, method B, results from the reaction of the ligand L with the heterotrimetallic linear complexes *trans*-$Pt[M(CO)_3Cp]_2(PhCN)_2$. The synthesis and charac-

(1) Organometallic Complexes with Metal–Metal Bonds. 19. Part 18: Bender, R.; Braunstein, P.; Jud, J. M.; Dusausoy, Y. *Inorg. Chem.* **1983**, *22*, 3394. Many publications have appeared since 1982, which were no longer numbered.
(2) (a) Université Louis Pasteur. (b) Université de Nancy.
(3) (a) Gladfelter, W. L.; Geoffroy, G. L. *Adv. Organomet. Chem.* **1980**, *18*, 207. (b) Roberts, D. A.; Geoffroy, G. L. In "Comprehensive Organometallic Chemistry"; Wilkinson, G., Stone, F. G. A., Abel, E. W., Eds.; Pergamon Press: Oxford, 1982; Chapter 40.
(4) Vahrenkamp, H. *Adv. Organomet. Chem.* **1983**, *22*, 169.
(5) Stone, F. G. A. *Acc. Chem. Res.* **1981**, *14*, 318; *Angew. Chem., Int. Ed. Engl.* **1984**, *23*, 89.
(6) Bender, R.; Braunstein, P.; Dusausoy, Y.; Protas, J. *J. Organomet. Chem.* **1979**, *172*, C51.

0020-1669/84/1323-4489$01.50/0

terization of the latter complexes are also given. Method B will be systematically compared in efficiency (cluster yield) with method A, since the same clusters are obtained by these two routes. Rational pathways are suggested for the reaction mechanisms.

Results and Discussion of the Syntheses

The general reaction of group 6 carbonylmetalate anions with *cis*- or *trans*-$PtCl_2L_2$ complexes in THF is shown in eq 1 and 2.

$$2PtCl_2L_2 + 2Na^+m^- \xrightarrow{THF} \begin{matrix} & L & \\ & \downarrow & \\ m & -Pt- & m \\ & \uparrow & \\ & L & \end{matrix} + 2NaCl \qquad (1)$$

m	PhCN	*t*-BuNC	c-$C_6H_{11}NC$
$Cr(CO)_3Cp$	**1a**	**1b**	**1c**
$Mo(CO)_3Cp$	**2a**		
$W(CO)_3Cp$	3a		
$Mn(CO)_5$	4a		

$$2PtCl_2(PR_3)_2 + 4Na^+[M(CO)_3Cp]^- \xrightarrow{THF} Pt_2M_2Cp_2(CO)_6(PR_3)_2 + 4NaCl + \ldots \qquad (2)$$

M = Cr, Mo, W; R = Et, Ph

Depending on the ligand L, this chemical route leads either to the formation of linear heterotrimetallic complexes (eq 1) or to the planar heterotetrametallic $Pt_2M_2Cp_2(CO)_6(PR_3)_2$ clusters (eq 2). The synthesis of the latter complexes according to eq 2 is called method A.

A second type of synthesis is discussed and deals with the reaction of tertiary phosphines, PR_3, or of CO with the linear heterotrimetallic benzonitrile complexes obtained in reaction 1. These reactions are represented by the equations (3)–(5).

$$2\ trans\text{-}Pt[M(CO)_3Cp]_2(PhCN)_2 + 2PR_3 \rightarrow Pt_2M_2Cp_2(CO)_6(PR_3)_2 + \ldots \qquad (3)$$

M	PMe_3	PEt_3	P-*n*-Bu_3	PPh_3
Cr		5f	5g	5h
Mo	6e	6f	6g	6h
W	7e	7f	7g	7h

$$5\ trans\text{-}Pt[Mn(CO)_5]_2(PhCN)_2 + 4PPh_3 \rightarrow Pt_5(CO)_6(PPh_3)_4 + \ldots \qquad (4)$$

$$trans\text{-}Pt[Mn(CO)_5]_2(PhCN)_2 + 2CO \rightarrow trans\text{-}Pt[Mn(CO)_5]_2(CO)_2 + 2PhCN \qquad (5)$$

4d

Thus, reaction 3 also leads to the $Pt_2M_2Cp_2(CO)_6(PR_3)_2$ clusters and is referred to as method **B** in the following.

Let us first consider the preparation of the trimetallic linear complexes.

A. Synthesis of the *trans*-Ptm_2L_2 Complexes. Many heterotrimetallic compounds of this type are now known (see previous papers in this series).[7,8] For example, the reaction of *trans*-$PdCl_2(py)_2$ with carbonylmetalates, m^-, such as $Co(CO)_4^-$, $Mn(CO)_5^-$, and $Mo(CO)_3Cp^-$ affording *trans*-$Pdm_2(py)_2$ complexes led to the first complexes containing metal–metal bonds between Pd and another transition metal.[7b] Further examples of complexes having a *trans*-Ptm_2L_2 structure with m = $Co(CO)_4$, $Co(CO)_3PPh_3$, $Fe(CO)_3NO$, $Mn(CO)_5$, $Mo(CO)_3Cp$, and $W(CO)_3Cp$ and L = *t*-BuNC and $C_6H_{11}NC$ have been described and were the first heteropolymetallic complexes with isocyanide ligands.[8]

We were interested in extending the latter series to m = $Cr(CO)_3Cp$ to see whether unbridged Pt–Cr bonds would be strong enough to allow the isolation of the linear *trans*-$Pt[Cr(CO)_3Cp]_2L_2$ complexes. This was also part of a study on the electrochemical reactivity of the metal–metal bonds in a series of related linear trimetallic complexes.[9] As expected, reaction 1 afforded the desired Cr–PtL_2–Cr complexes **1b** and **1c**. (See details in the Experimental Section and in Table IV, supplementary material.)

There is no definitive example of a linear trimetallic complex of the type mentioned above where the two ligands L attached to the central metal are tertiary phosphines. Previous results on the reaction of tertiary phosphines, PR_3, with linear trimetallic Co–PtL_2–Co or Fe–PtL_2–Fe complexes[8,10] have shown that rupture of the metal–metal bonds occurs, affording ionic complexes, instead of a CO substitution reaction, like in the corresponding Co–Hg–Co[11] or Fe–Hg–Fe[12] complexes. Furthermore, attempts to prepare such complexes by reactions of the type shown in eq 2 inevitably lead to ligand redistribution and cluster formation (see below; method A). This failure could be assigned to either electronic or steric effects. We were inclined to invoke the latter, and this has been recently supported by the isolation of the bimetallic $(PPh_3)_2HPtMo(CO)_3Cp$ complex, in which the steric constraint about the platinum is relieved by the small hydrido ligand, now allowing the two PPh_3 ligands to remain coordinated to platinum.[13]

We were interested in attempting the preparation of linear trimetallic complexes containing the labile PhCN ligands on platinum (eq 1). Indeed, these molecules could now react with PR_3 ligands in a different manner: by replacement of one or two PhCN ligands. This, in turn, could either lead to the so far unknown linear m–$Pt(PR_2)_2$–m complexes or induce a fragmentation of the framework, if the steric constraints were too large.

The desired trimetallic complexes **1a–4a** were prepared according to eq 1 (see Experimental Section), indicating that, in $PtCl_2(PhCN)_2$, Cl^- is a better leaving group than PhCN vs. the carbonylmetalate anions. These complexes are much more stable than their palladium analogues, which could be prepared but not isolated in the solid state.[1]

The successful preparation of the m–PtL_2–m complexes **1a–4a** originates from the presence on Pt of nonsterically demanding ligands. The same reason applied when these ligands were pyridine or substituted pyridines,[7] isocyanides,[8] or CO.[14] We shall see below (method B) that it is indeed impossible to accommodate two bulky ligands on platinum in such complexes.

B. Clusters: Synthetic Method A. We have alluded above to the fact that changing the ligand L in *trans*-$PtCl_2L_2$ from pyridine to tertiary phosphines dramatically changes the course of the reaction of these complexes with $Na[M(CO)_3Cp]$ (M = Cr, Mo, W). Indeed, instead of the linear trimetallic complexes isolated with pyridine[7] or isocyanides,[8] for example, new types of clusters are formed, which are the subject of this paper. Analogous observations have already been made with other carbonylmetalates such as $Co(CO)_4^-$,[15,16] $Fe(CO)_3NO^-$,[17]

(7) (a) Braunstein, P.; Dehand, J. *J. Organomet. Chem.* **1970**, *24*, 497. (b) *C. R. Hebd. Seances Acad. Sci., Ser. C* **1972**, *274*, 175. (c) *J. Organomet. Chem.* **1974**, *81*, 123. (d) *Bull. Soc. Chim. Fr.* **1975**, 1997.
(8) Barbier, J. P.; Braunstein, P. *J. Chem. Res., Synop.* **1978**, 412; *J. Chem. Res., Miniprint* **1978**, 5029.
(9) Lemoine, P.; Giraudeau, A.; Gross, M.; Braunstein, P. *J. Chem. Soc., Chem. Commun.* **1980**, 77.
(10) Pearson, R. G.; Dehand, J. *J. Organomet. Chem.* **1969**, *16*, 485.
(11) Hieber, W.; Breu, R. *Chem. Ber.* **1957**, *90*, 1259. King, R. B. *Inorg. Chem.* **1963**, *2*, 936. Bonati, F.; Cenini, S.; Ugo, R. *J. Chem. Soc. A* **1967**, 932.
(12) King, R. B. *Inorg. Chem.* **1963**, *2*, 1275. Hieber, W.; Klingshirn, W. *Z. Anorg. Allg. Chem.* **1963**, *323*, 292.
(13) Bars, O.; Braunstein, P. *Angew. Chem., Int. Ed. Engl.* **1982**, *94*, 319.
(14) (a) Braunstein, P.; Matt, D.; Bars, O.; Grandjean, D. *Angew. Chem., Int. Ed. Engl.* **1979**, *18*, 797. (b) Bars, O.; Braunstein, P.; Jud, J. M. *Nouv. J. Chim.*, in press.
(15) Braunstein, P.; Dehand, J.; Nennig, J. F. *J. Organomet. Chem.* **1975**, *92*, 117.
(16) Barbier, J. P.; Braunstein, P.; Fischer, J.; Ricard, L. *Inorg. Chim. Acta* **1978**, *31*, L361.

or $Mn(CO)_5^-$,[18] where tetra- or pentametallic clusters were formed. With the carbonylmetalates used in this work, the heterotetrametallic $Pt_2M_2Cp_2(CO)_6(PR_3)_2$ clusters were obtained. This is very similar to what we observed with palladium in place of platinum.[1] A preliminary report has been published on the clusters **6f**, **6h**, **7f**, and **7h**.[6] The formation of clusters with PR_3 ligands originates from the impossibility to make the linear m–$Pt(PR_3)_2$–m complexes: the steric bulk of the phosphines strongly destabilizes such a structure (see below; method B), and the phosphine lability accounts for the presence of only one PR_3 ligand coordinated to Pt in the final clusters.

Typically, the reaction products were separated by column chromatography, and this will also apply to method B (details in the Experimental Section). In the following, we will always refer to isolated products *after* chromatography and we recognize that some secondary reactions may occur on the column.[19] The principal reaction products isolated are $Pt_2M_2Cp_2(CO)_6(PR_3)_2$, $Pt_5(CO)_6(PR_3)_4$,[18] and $[M(CO)_3Cp]_2$. In some syntheses, we also isolated smaller quantities of $Cr_2(CO)_4Cp_2$,[20] $Mo_2(CO)_5(PPh_3)Cp_2$,[21] $MoCp(CO)_2(PPh_3)Cl$,[22] and *trans*-$Pt(H)Cl(PR_3)_2$ (R = Et,[23] Ph[24,25]). The latter is unlikely to be present already in the reaction mixture since we have independently shown that *trans*-$Pt(H)Cl(PPh_3)_2$ reacts very rapidly with $Mo(CO)_3Cp^-$ to give the bimetallic $(PPh_3)_2(H)PtMo(CO)_3Cp$ complex.[13] Therefore, this hydrido complex most probably forms on the chromatography column. We also established that $Pt_3(CO)_3(PPh_3)_4$ can be transformed into $Pt_5(CO)_6(PPh_3)_4$ upon chromatography.[19] In the synthesis of **5h**, however, we have isolated $Pt_5(CO)_6(PPh_3)_4$ directly, without chromatographic separation (see Experimental Section).

The nature of the observed products supports the reaction mechanisms proposed in our previous paper[1] concerning the palladium analogues of the Pt_2M_2 clusters discussed here. For sake of clarity, we shall briefly describe the different steps envisaged. It is reasonable to assume that the first step in reaction 2 is the substitution of one chloride by the carbonylmetalate anion.[7a]

The second step, analogous to what occurs in reaction 1, would then lead to the highly unstable m–$Pt(PR_3)_2$–m intermediate (vide supra). In order to explain the formation of the reaction products observed, we think that this intermediate must rapidly fragment into radicals such as $[Cp(OC)_3M–Pt(PR_3)_2]\cdot$ and $[M(CO)_3Cp]\cdot$ or $Pt(PR_3)_2$ and $[M(CO)_3Cp]\cdot$. The heterobimetallic radical could further lose a phosphine ligand and dimerize into the observed $Pt_2M_2Cp_2(CO)_6(PR_3)_2$ clusters. In support of this, we have recently shown that radicals such as $[Cp(OC)_3M–Pt(CNR)_2]\cdot$ or $[(OC)_4Co–Pt(PR_3)]\cdot$ can be electrochemically generated[9,26] and, in the latter case, dimerize into the known $Pt_2Co_2(CO)_8(PPh_3)_2$ cluster.[15] The $Cp(OC)_2Cr{\equiv}Cr(CO)_2Cp$ complex observed in the synthesis of **5f** could originate either from the dimerization of a $[Cr(CO)_2Cp]\cdot$ radical (easily formed from $[Cr(CO)_3Cp]\cdot$) or from $[Cr(CO)_3Cp]_2$. The latter is known to easily lose 2 mol of CO (either in solution[20] or on column chromatography) or generate the $[Cr(CO)_3Cp]\cdot$ radical.[27]

The combination of some unsaturated 14-electron Pt(0) fragments such as $Pt(PR_3)_2$, $Pt(CO)(PR_3)$, or $Pt(CO)_2$ would account for the formation of the $Pt_5(CO)_6(PR_3)_4$ clusters.[28]

These radical and fragment recombinations are presented in the reaction mechanism suggested for method B, as illustrated in Scheme I.

Scheme I[a]

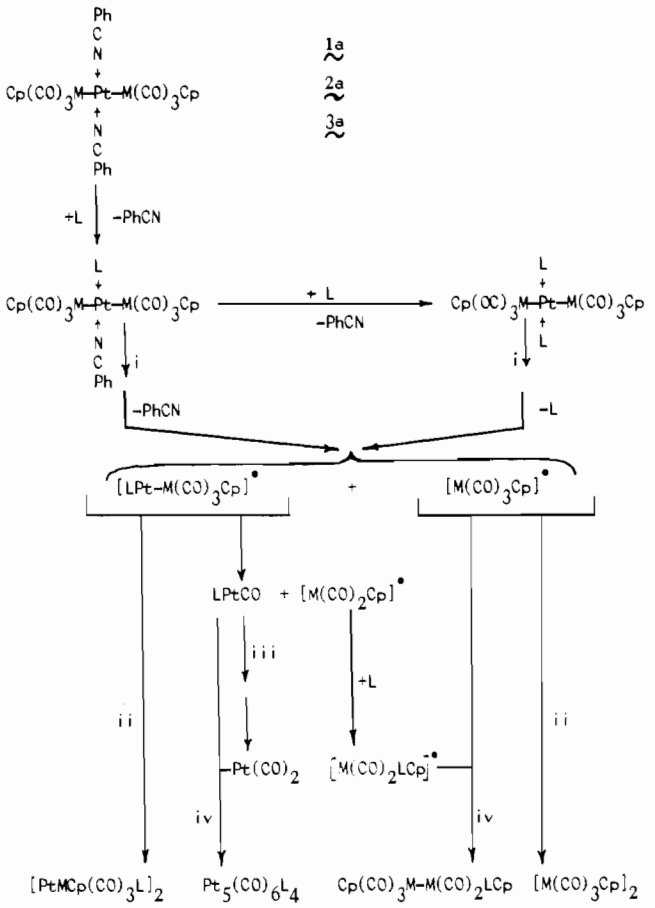

[a] Key: (i) homolytic cleavage; (ii) radical dimerization; (iii) ligand exchange; (iv) fragment condensation.

(17) Bender, R.; Braunstein, P.; Fischer, J.; Ricard, L.; Mitschler, A. *Nouv. J. Chim.* **1981**, *5*, 81.
(18) Barbier, J. P.; Bender, R.; Braunstein, P.; Fischer, J.; Ricard, L. *J. Chem. Res., Synop.* **1978**, 230; *J. Chem. Res., Miniprint* **1978**, 2913.
(19) Bender, R.; Braunstein, P. *J. Chem. Soc., Chem. Commun.* **1983**, 334.
(20) Ginley, D. S.; Bock, C. R.; Wrighton, M. S. *Inorg. Chim. Acta* **1977**, *23*, 85.
(21) (a) Barnett, K. W.; Treichel, P. M. *Inorg. Chem.* **1967**, *6*, 294. (b) Haines, R. J.; Nyholm, R. S.; Stiddard, M. H. B. *J. Chem. Soc. A* **1968**, 43.
(22) Treichel, P. M.; Barnett, K. W.; Shubkin, R. L. *J. Organomet. Chem.* **1967**, *7*, 449.
(23) Chatt, J.; Duncanson, L. A.; Shaw, B. L.; Venanzi, L. M. *Discuss. Faraday Soc.* **1958**, *26*, 131.
(24) Chatt, J.; Shaw, B. L. *J. Chem. Soc.* **1962**, 5075.
(25) A preliminary X-ray structural determination has been carried out on single crystals of *trans*-$Pt(H)(Cl)(PPh_3)_2$ obtained from THF/pentane. The poor quality of the crystals has not allowed the final resolution of the structure. Preliminary crystal data: $C_{36}H_{31}ClP_2Pt$, triclinic, space group $P\bar{1}$; a = 18.38 (1), b = 9.65 (1), c = 20.60 (1) Å; Z = 2. A structural disorder along the parameter a was found. An approximate structure resolution has been made on the reduced unit cell with a = 9.19 Å, using Patterson and Fourier methods to R = 0.11 for 2769 unique data [$I > \sigma(I)$], all atoms being assigned isotropic thermal parameters. The platinum atom has a square-planar trans environment: Pt–P(1) = 2.30 (1), Pt–P(2) = 2.15 (2), Pt–Cl = 2.36 (1) Å; P(1)–Pt–P(2) = 173 (1), P(1)–Pt–Cl = 93 (1), P(2)–Pt–Cl = 91 (1)°.
(26) Lemoine, P.; Giraudeau, A.; Gross, M.; Bender, R.; Braunstein, P. *J. Chem. Soc., Dalton Trans.* **1981**, 2059.
(27) Madach, T.; Vahrenkamp, H. *Z. Naturforsch., B: Anorg. Chem., Org. Chem.* **1978**, *33B*, 1301.
(28) Preliminary experiments have shown that when reaction 2 was carried out in the presence of free PPh_3 (with $PPh_3/Pt(PPh_3)_2Cl_2$ = 4), no Pt_2M_2 cluster was formed and instead mononuclear complexes were dramatically favored. The predominant complexes isolated were $Mo(CO)_2(PPh_3)CpCl$, *trans*-$Pt(H)Cl(PPh_3)_2$ (ca. 16% yield) and $Pt(PPh_3)_{3or4}$ (ca. 59% yield), supporting the intermediacy of mononuclear unsaturated fragments in this reaction. The presence of free PPh_3, by stabilizing this intermediates, deviates the reaction route of cluster formation. These complexes were separated by column chromatography (silica gel) using pentane/toluene. Chlorinated solvents may lead to side reactions during chromatography, as reported with the formation from a molybdenum precursor and CH_2Cl_2 of the chloro complex $Mo(CO)_2(PPh_3)CpCl$.[29]
(29) Endrich, K.; Korswagen, R.; Zahn, T.; Ziegler, M. L. *Angew. Chem. Suppl.* **1982**, 1906.

It is clear that the lifetime and the reactivity of the above-mentioned species will depend upon the nature of both the metal M and the ligand PR_3. For example, competition is clearly found between the formation of the cluster $Pt_2Cr_2Cp_2(CO)_6(PR_3)_2$ and of $Pt_5(CO)_6(PR_3)_4$ (see Experimental Section), even to the point that no $Pt_2Cr_2Cp_2(CO)_6(PPh_3)_2$ could be obtained by method A but instead a relatively increased yield of $Pt_5(CO)_6(PPh_3)_4$ (27%) (see Table VI, supplementary material).

At this stage, it is interesting to remember that the reaction of *trans*-$PtCl_2(PPh_3)_2$ with $NaMn(CO)_5$ afforded $Pt_5(CO)_6(PPh_3)_4$ as the only isolated cluster.[18] No mixed Pt–Mn cluster was found in this synthesis. Furthermore, the obtention in the latter reaction of $Mn_2(CO)_9(PPh_3)$ and $Mn_2(CO)_8(PPh_3)_2$, under very mild conditions (such that direct thermal substitution of phosphine for CO in $Mn_2(CO)_{10}$ is precluded[30,31]), again favors the involvement of radical[32] pathways in the general redox reaction of $PtCl_2(PR_3)_2$ complexes with carbonylmetalate anions.

C. Clusters: Synthetic Method B. As justified above in this paper, we considered it of interest to look at the reactivity of the trimetallic linear complexes m–$Pt(PhCN)_2$–m with tertiary phosphines. We have found that the substitution of the PhCN ligands in these complexes is accompanied by a rupture of the metal–metal bond(s) and results in the formation of clusters. It is important to realize that since these clusters are the same as those obtained by method A, a valuable comparison will become possible between these two synthetic methods.

Typically, the trimetallic *trans*-$Pt[M(CO)_3Cp]_2(PhCN)_2$ (M = Cr, Mo, W) were reacted with 1 equiv of PR_3 in THF. The reaction occurs slowly at room temperature for M = W whereas heating under reflux for several hours is necessary for M = Cr and Mo (details in the Experimental Section and in Table VII, supplementary material).

The identified products isolated after purification are essentially the clusters $Pt_2M_2Cp_2(CO)_6(PR_3)_2$ and $Pt_5(CO)_6(PR_3)_4$,[18] $[M(CO)_3Cp]_2$, and the new $Mo_2(CO)_5(PMe_3)Cp_2$ (analogous to the PEt_3-[1] and PPh_3-substituted[21] dimers).

Scheme I summarizes possible pathways to account for the formation of these complexes.

Complexes **1a**, **2a**, and **3a** are only sparingly soluble in THF, in contrast to the PR_3 ligands. Despite the fact that the overall phosphine to platinum stoichiometry is only 1:1, the local concentration of PR_3 is therefore much higher than that of the dissolved trimetallic complexes. This justifies the hypothesis of the intermediate formation of *trans*-$Pt[M(CO)_3Cp]_2(PR_3)_2$ (Scheme I). The fragmentation of this species occurs, as described under method A, with liberation of one PR_3 ligand.

For the sake of completeness, and without kinetic data to differenciate among the various possibilities, we also include in Scheme I the possible intermediacy of *trans*-$Pt[M(CO)_3Cp]_2(PhCN)(PR_3)$. This would bear an analogy with the formation of the complex $PtCl_2(PhCN)(P\text{-}t\text{-}Bu_3)$ from $PtCl_2(PhCN)_2$ and P-*t*-Bu_3 in a 1:1 molar ratio.[33] The known reactivity of the $[M(CO)_3Cp]\cdot$ radicals[34] explains their easy phosphine substitution for CO and/or their dimerization. To account for the formation of the unsaturated $Pt(CO)(PR_3)$ and $Pt(CO)_2$ fragments, we favor a concerted CO transfer from M to Pt in a metal–metal-bonded intermediate. Related situations have been found with Ni–M intermediates.[35]

The observed competition between the formation of the mixed-metal clusters Pt_2M_2 and of Pt_5 in these syntheses is particularly striking in the cases of M = Cr and Mo with L = PPh_3. In the former case, 63% of the platinum is found in the form of the Pt_5 and 3% in the form of the Pt_2Cr_2 cluster, whereas with Mo the yields in Pt_5 and Pt_2Mo_2 are respectively 0% and 87%. An explanation would be that steric hindrance about platinum in the possible intermediate *trans*-$Pt[M(CO)_3Cp]_2(PR_3)_2$ is higher for M = Cr than for M = Mo or W because of shorter metal–metal bonds in the former case, resulting in the easy rupture of both Pt–Cr bonds and in the formation of a stable *homo*nuclear platinum cluster.

In general, we find that method B requires more vigorous reaction conditions than method A but affords slightly better yields in the mixed $Pt_2M_2Cp_2(CO)_6(PR_3)_2$ clusters and much better yields in platinum-containing complexes (including now $Pt_5(CO)_6(PR_3)_4$).

For comparison with the above-described reactions, we prepared the complex *trans*-$Pt[Mn(CO)_5]_2(PhCN)_2$ (**4a**) and investigated its reactivity toward PPh_3 and CO (eq 4, 5).

The reaction of **4a** with PPh_3 (see Experimental Section) resulted in a 70% yield of $Pt_5(CO)_6(PPh_3)_4$, after optimization of the phosphine to platinum ratio at 4:5. This result is consistent with the fact that reaction of $PtCl_2(PPh_3)_2$ with $NaMn(CO)_5$ also leads to this Pt_5 cluster and not to a mixed Pt–Mn one.[18] This does not originate from a particularly weak Pt–Mn bond[7c,14b] but most certainly from the fact that, in both reactions, the intermediate *trans*-$Pt[Mn(CO)_5]_2(PPh_3)_2$ collapses rapidly for steric reasons. This occurs with rupture of the Pt–Mn bonds, liberating platinum-containing fragments that prefer to combine with each other rather than with manganese-containing fragments.

When the reaction of **4a** with PPh_3 was performed under CO, a lower yield of $Pt_5(CO)_6(PPh_3)_4$ was obtained (46%) but a new, poorly soluble complex was formed (11%), which is formulated as $[Pt(CO)(PPh_3)]_n$ (ν(CO) = 1800 cm^{-1})[36a] on the basis of analytical data (see Experimental Section). Furthermore, the complex *trans*-$Pt[Mn(CO)_5]_2(CO)_2$ (**4d**) was isolated in 25% yield. This complex was independently shown not to react with PPh_3 under similar reaction conditions. Thus, competition between PPh_3 and CO clearly occurs for PhCN substitution in **4a**.

Finally, when CO was bubbled (at room temperature and atmospheric pressure) into a toluene solution of **4a**, **4d** was formed and isolated in 90% yield (eq 5). This complex had been obtained previously in very low yield from the reaction of *trans*-$PtCl_2(PPh_2Cl)_2$ with $NaMn(CO)_5$.[14,36b]

This clearly indicates that in **4d** the CO ligands can easily be accommodated in the platinum coordination sphere with retainment of the Mn–Pt–Mn array[14b] whereas the bulky PR_3 ligands cannot. Under similar conditions, complexes **1a**, **2a**, and **3a** did not react with CO.

D. Spectroscopic Characterization. The infrared spectral data for the trimetallic complexes are given in Table I. The ν(CN) absorption band is only observed in **1b** and **1c**. The ν(CO) absorptions are very similar both in frequencies and in intensities to those reported for the corresponding m–PtL_2–m complexes where L = pyridine or isocyanides.[7,8] The ν(PtM) asymmetric vibration gives rise to a strong absorption in a region of the far-IR where other vibrations are absent.[7,8,37] Thus, the values of 173, 174, and 177 cm^{-1} for **1a**–**1c**, re-

(30) Osborne, A. G.; Stiddard, M. H. B. *J. Chem. Soc.* **1964**, 634.
(31) Haines, L. I. B.; Hopgood, D.; Poë, A. J. *J. Chem. Soc. A* **1968**, 421.
(32) Poë, A. *Inorg. Chem.* **1981**, *20*, 4029. Atwood, J. D. *Inorg. Chem.* **1981**, *20*, 4031 and references cited.
(33) Clark, H. C.; Goel, A. B.; Goel, R. G.; Goel, S. *Inorg. Chem.* **1980**, *19*, 3220.
(34) See for example ref 21a and: Alway, D. G.; Barnett, K. W. *Inorg. Chem.* **1980**, *19*, 1533. Hoffman, N. W.; Brown, T. L. *Inorg. Chem.* **1978**, *17*, 613.
(35) Braunstein, P.; Dehand, J.; Munchenbach, B. *J. Organomet. Chem.* **1977**, *124*, 71.
(36) (a) Bender, R. Thèse de Doctorat ès Sciences Physiques, Université Louis Pasteur, Strasbourg, 1979. (b) Braunstein, P.; Matt, D.; Bars, O.; Louër, M.; Grandjean, D.; Fischer, J.; Mitschler, A. *J. Organomet. Chem.* **1981**, *213*, 79.
(37) Braunstein, P.; Schubert, U.; Burgard, M. *Inorg. Chem.*, in press.

Table I. Infrared Spectral Data for the Linear Trimetallic Complexes

complex	IR abs max,[a] cm^{-1} ν(CO) KBr	ν(CO) Nujol	ν(CN) KBr	ν(CN) Nujol	ν(PtM)[b] polythene
trans-Pt[Cr(CO)$_3$Cp]$_2$(PhCN)$_2$ (**1a**)	1884 s, 1840 s, 1808 s	1883 s, 1839 s, 1808 s			173 s
trans-Pt[Mo(CO)$_3$Cp]$_2$(PhCN)$_2$ (**2a**)	2054 w, 1900 s, 1862 sh, 1834 s br	2053 w, 1994 w, 1979 w, 1904 s, 1854 s sh, 1833 s br			148 s
trans-Pt[W(CO)$_3$Cp]$_2$(PhCN)$_2$ (**3a**)	2060 vw, 1900 s, 1861 sh, 1832 s	2051 w, 1975 vw, 1906 s, 1836 s br			134 m
trans-Pt[Mn(CO)$_5$]$_2$(PhCN)$_2$ (**4a**)	2023 s, 1974 s, 1949 vw, 1926 s	2027 s, 1968 s br, 1949 vw, 1927 s			157 vs
trans-Pt[Cr(CO)$_3$Cp]$_2$(*t*-BuNC)$_2$ (**1b**)	1895 s, 1855 s, 1825 s		2185 s		174 s
trans-Pt[Cr(CO)$_3$Cp]$_2$(C$_6$H$_{11}$NC)$_2$ (**1c**)	1902 s, 1838 s, 1811 ms	1902 ms, 1838 vs, 1811 s	2190 s	2190 s	177 s
trans-Pt[Mn(CO)$_5$]$_2$(CO)$_2$ (**4d**)	2058 s, 2040 s, 2017 s, 1985 vs, 1962 vs br	2062 ms, 2042 ms, 2017 ms, 1981 s sh, 1971 vs			171 s

[a] Abbreviations: s, strong; m, medium; w, weak; sh, shoulder; br, broad. [b] Other absorptions at 114 s and 98 vs cm^{-1} for **3a** and **4d**, respectively.

Table II. Infrared Spectral Data for the Cluster Complexes

complex	IR abs max,[a] cm^{-1} [ν(CO)] KBr	Nujol
$Pt_2Mo_2Cp_2(CO)_6(PMe_3)_2$ (**6e**)	1813 s, 1708 s	1818 s, 1795 sh, 1720 s
$Pt_2W_2Cp_2(CO)_6(PMe_3)_2$ (**7e**)	1806 s, 1691 s	1804 vs, 1697 s
$Pt_2Cr_2Cp_2(CO)_6(PEt_3)_2$ (**5f**)	1818 vs, 1758 s, 1731 s	1818 vs, 1779 m, 1760 sh, 1746 s, 1733 sh
$Pt_2Mo_2Cp_2(CO)_6(PEt_3)_2$ (**6f**)	1816 sh, 1805 s, 1722 sh, 1706 s	1818 s, 1806 s, 1784 m sh, 1739 ms, 1711 vs
$Pt_2W_2Cp_2(CO)_6(PEt_3)_2$ (**7f**)	1848 m sh, 1793 s, 1734 w, 1687 s	1858 mw, 1815 sh, 1786 s, 1748 w, 1686 s
$Pt_2Cr_2Cp_2(CO)_6(P\text{-}n\text{-}Bu_3)_2$ (**5g**)	1812 vs, 1754 sh, 1735 s	
$Pt_2Mo_2Cp_2(CO)_6(P\text{-}n\text{-}Bu_3)_2$ (**6g**)	1893 m sh, 1801 s, 1722 sh, 1703 s	1842 m sh, 1800 s, 1731 sh, 1703 s
$Pt_2W_2Cp_2(CO)_6(P\text{-}n\text{-}Bu_3)_2$ (**7g**)	1837 sh, 1797 s, 1689 s	
$Pt_2Cr_2Cp_2(CO)_6(PPh_3)_2$ (**5h**)	1821 s, 1783 m, 1757 s	
$Pt_2Mo_2Cp_2(CO)_6(PPh_3)_2$ (**6h**)	1831 s, 1798 m sh, 1753 sh, 1739 s	1831 s, 1797 m, 1751 sh, 1741 s
$Pt_2W_2Cp_2(CO)_6(PPh_3)_2$ (**7h**)	1823 s, 1786 m sh, 1723 s	1826 s, 1798 m sh, 1726 s

[a] Abbreviations: s, strong; m, medium; w, weak; sh, shoulder; br, broad.

spectively, are the first reported for a Pt–Cr vibration. The frequencies found for the other complexes are in the same range as those observed in similar trimetallic systems.[7,8]

The infrared spectral data in the ν(CO) region are given for all mixed-metal clusters in Table II. Considering their X-ray structures (see Figures 2 and 3), the very strong absorption between ca. 1750 and 1690 cm^{-1} is assigned to the ν(CO) vibration of the triply bridging C(2)–O(2) ligand, whereas the absorptions between ca. 1800 and 1900 cm^{-1} are assigned to the vibrations of the semibridging C(1)–O(1) and C(3)–O(3) ligands. An increase in the basicity of the phosphine ligand generally induces a decrease in the ν(CO) frequencies, reflecting an increased π back-donation from the metals toward the carbonyl ligands.

The ^{1}H, ^{31}P, and ^{13}C NMR data for the clusters are collected in Table III. In ^{1}H NMR spectroscopy, the η^5-C$_5$H$_5$ protons are equivalent and appear as a singlet (^4J(PH) = 0 Hz, as in the palladium analogues[1]) with ^{195}Pt satellites (^3J(PtH) $\sim$ 4 Hz).[38]

The PMe$_3$ protons of **6e** and **7e** give rise to a singlet. The "virtual coupling" usually observed along the linear R$_3$P–Pt–Pt–PR$_3$ arrangement (see Table III) is found in this instance to be $|^2J(PH) + {}^5J(PH)| \sim 0$ Hz. The ^{195}Pt satellites of the isotopomer with one ^{195}Pt (I = $^1/_2$; 44.68% abundance) were observed. These lines are centered 1.5 Hz downfield from the singlet due to the resonance for the isotopomer containing no ^{195}Pt (43.95% abundance) (isotopic chemical shift).

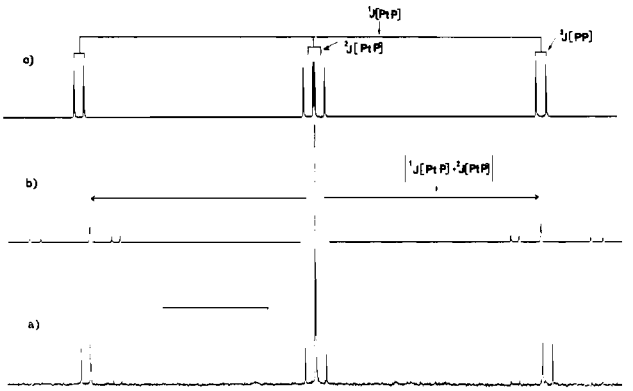

Figure 1. ^{31}P coupling scheme observed for **6g** and **7g**: (a) experimental spectrum (the bar represents 1000 Hz); (b) calculated spectrum for AA′ part of the AA′XX′ spin system (11.35% abundance); (c) calculated spectrum for the AA′ part of the AA′X spin system (44.68% abundance).

The CH$_2$ protons of PEt$_3$ (complexes **6f** and **7f**) appear as a doublet of quadruplets owing to coupling with CH$_3$ protons and with phosphorus. The CH$_3$ protons show a doublet of triplets owing to coupling with CH$_2$ protons and with phosphorus.

For all complexes, the ^{31}P{^{1}H} NMR (Table III) confirms in solution the equivalence found in the solid state (vide infra) for the phosphine ligands. The chemical shifts measured for **6e**, **7e**; **6f**, **7f**; and **6g**, **7g** are downfield of *trans*-PtCl$_2$(PMe$_3$)$_2$ (−15.8 ppm[39]), *trans*-PtCl$_2$(PEt$_3$)$_2$ (12.1 ppm[39]), and *trans*-

(38) Spectra derived from polynuclear platinum complexes are complicated by the presence of a mixture of isotopomers. These arise from the differing isotopic distributions of ^{195}Pt, $I = {}^1/_2$, natural abundance 33.7%. For a centrosymmetric R$_3$P–Pt–Pt–PR$_3$ arrangement, the three isotopomers are in relative abundance as follows: R$_3$P–Pt–Pt–PR$_3$ (I), 43.95%; R$_3$P–Pt*–Pt–PR$_3$ (or R$_3$P–Pt–Pt*–PR$_3$) (II), 44.68%; R$_3$P–Pt*–Pt*–PR$_3$ (III), 11.35%. The most intense features are therefore observed for species I and II. For the η^5-C$_5$H$_5$ protons, for example, the singlet due to species I overlaps with the central line of the triplet assigned to III, giving rise to a typical 1:8:18:8:1 pattern including the doublet originating from species II.

(39) Favez, R.; Roulet, R.; Pinkerton, A. A.; Schwarzenbach, D. *Inorg. Chem.* **1980**, *19*, 1356.

Table III. ^1H, $^{31}P\{^1H\}$, and $^{13}C\{^1H\}$ NMR Spectral Data[a-c]

complex	δ		
	^1H	$^{31}P\{^1H\}$	$^{13}C\{^1H\}$
$Pt_2Mo_2Cp_2(CO)_6(PMe_3)_2$ (6e)	*5.25 (s, 10 H, C_5H_5, $^3J(PtH) = 4.1$), 1.53 (s, 18 H, MeP, $\|^2J(PH) + {}^5J(PH)\| < 1$)[d]	*5.15 (s)	
$Pt_2W_2Cp_2(CO)_6(PMe_3)_2$ (7e)	*5.34 (s, 10 H, C_5H_5, $^3J(PtH) = 5.0$), 1.51 (s, 18 H, MeP, $\|^2J(PH) + {}^5J(PH)\| < 1$)[d]	*4.13 (s)	
$Pt_2Mo_2Cp_2(CO)_6(PEt_3)_2$ (6f)	*5.27 (s, 10 H, C_5H_5, $^3J(PtH) = 3.4$), 1.90 (dq, 12 H, CH_2CH_3),[e] 0.99 (dt, 18 H, CH_2CH_3)[f]	*40.9 (s, $^3J(PP) = 91$, $^1J(PtP) = 4402$, $^2J(PtP) = -107$)	*243.2 (s, CO, $J(PtC) = 80$), 91.8 (s, C_5H_5), m centered at 17.1 (CH_2CH_3), 8.30 (s, CH_2CH_3)
$Pt_2W_2Cp_2(CO)_6(PEt_3)_2$ (7f)	*5.35 (s, 10 H, C_5H_5, $^3J(PtH) = 4.6$), 1.85 (dq, 12 H, CH_2CH_3),[e] 0.95 (dt, 18 H, CH_2CH_3)[f]	*43.2 (s, $^3J(PP) = 92$, $^1J(PtP) = 4582$, $^2J(PtP) = -130$)	*89.7 (s, C_5H_5), m centered at 17.5 (CH_2CH_3), 8.04 (s, CH_2CH_3)
$Pt_2Mo_2Cp_2(CO)_6(P\text{-}n\text{-}Bu_3)_2$ (6g)	**5.23 (s, 10 H, C_5H_5, $^3J(PtH) = 3.8$), 1.8-0.8 (m, 54 H, *n*-Bu)	*33.6 (s, $^3J(PP) = 93$, $^1J(PtP) = 4397$, $^2J(PtP) = -106$, $J(PtPt) = 775$)	*243.4 (s, CO, $J(PtC) = 83$), 91.8 (s, C_5H_5, $J(PtC) = 31$), 26.5-24.3 (br m, $CH_2CH_2CH_2CH_3$), 13.7 (s, $CH_2CH_2CH_2CH_3$)
$Pt_2W_2Cp_2(CO)_6(P\text{-}n\text{-}Bu_3)_2$ (7g)	**5.31 (s, 10 H, C_5H_5, $^3J(PtH) = 4.7$), 2-0.4 (m, 54 H, *n*-Bu)	*32.4 (s, $^3J(PP) = 87$, $^1J(PtP) = 4424$, $^2J(PtP) = -103$, $J(PtPt) = 1039$)	*237.4 (s, CO, $J(PtC) = 58$), 89.8 (s, C_5H_5), 26.5-24.3 br m, $CH_2CH_2CH_2CH_3$), 13.7 (s, $CH_2CH_2CH_2CH_3$)
$Pt_2Mo_2Cp_2(CO)_6(PPh_3)_2$ (6h)	*4.73 (s, 10 H, C_5H_5, 7.47-7.42 (m, 30 H, C_6H_5)	*47.9 (s)	
$Pt_2W_2Cp_2(CO)_6(PPh_3)_2$ (7h)	*4.78 (s, 10 H, C_5H_5), 7.59-7.52 (m, 30 H, C_6H_5)	*49.3 (s)	

[a] Measured in CD_2Cl_2 (*) or in $CDCl_3$ (**) at room temperature. Coupling constants in Hz (see Experimental Section A). [b] ^{13}C NMR spectra not measured due to insufficient solubility. [c] Key: s, singlet; m, multiplet; d, doublet; t, triplet; q, quartet. [d] $^3J(PtH) = 36$, $^4J(PtH) \simeq 0$, $^2J(PH) = 10$, $^5J(PH) = 1$ Hz for the monolabeled ^{195}Pt complex. [e] $^3J(HH) = 7.5$, $|^2J(PH) + {}^5J(PH)| = 8.5$ Hz. [f] $^3J(HH) = 7.5$, $|^3J(PH) + {}^6J(PH)| = 17$ Hz.

$PtCl_2(P\text{-}n\text{-}Bu_3)_2$ (4.5 ppm[39]), respectively.

In four instances, **6f**, **7f**, **6g**, and **7g**, the ^{195}Pt satellites of the monolabeled complex[38] are clearly observed and show an AA'X spin system (A, A' = P; X = ^{195}Pt). The lines are centered about the chemical shift value of the unlabeled species. The lines of the AA' spectrum corresponding to small Pt–P coupling are interior to the ones with larger Pt–P coupling (see Figure 1 for **6g** or **7g**). Coupling constants are given in Table III.

In the $^{31}P\{^1H\}$ spectra of **6g** and **7g** we can further observe an AA'XX' pattern due to the doubly labeled ^{195}Pt isotopomer (see Figure 1). From the analysis of the lines of these two systems (AA'X and AA'XX') it must be emphasized that $|^1J(PtP) + {}^2J(PtP)|$ is smaller than $|^1J(PtP)| + |^2J(PtP)|$. We can therefore conclude that $^1J(PtP)$ and $^2J(PtP)$ are opposite in sign. From the position of the inner and outer lines in the AA'XX' spectrum, the value of $J(PtPt)$ is readily obtained and found to be 775 and 1039 Hz in **6g** and **7g**, respectively.

In the $^{13}C\{^1H\}$ NMR spectra (Table III), the cyclopentadienyl carbons give rise to a singlet. The ^{195}Pt satellites due to the monolabeled complex were only observed for **6g**. The lower solubility of the other complexes precluded their observation.

The carbon atoms of the PEt_3 and P-*n*-Bu_3 ligands in **6f**, **7f**, **6g**, and **7g** show complicated multiplets.

The carbonyl ligands when detected in the ^{13}C spectra always give rise at room temperature to a singlet between 237.4 and 243.2 ppm. These chemical shifts are similar to those reported for the anions $Cr(CO)_3Cp^-$ (246.7 ppm[40]) and $Mo(CO)_3Cp^-$ (236.2 ppm[41]). The singlet was still observed in the spectrum of **6g** at −30 °C (the other complexes were not soluble enough), indicating the equivalence of the CO ligands on the NMR time scale. The same has been found for the carbonyls of the related $Pd_2M_2Cp_2(CO)_6(PR_3)_2$ clusters.[1] ^{195}Pt satellites are observed with coupling constants of 80, 83, and 58 Hz for **6f**, **6g**, and **7g**, respectively. These coupling constants represent the algebraic sum of all possible contributions and are averaged over three carbonyls.

We can envisage the process that renders the carbonyls equivalent as a rapid rotation of the $M(CO)_3$ tripod about its C_3 axis.[1] During this process, the CO ligands would always "see" the platinum atoms of the cluster. We think that in the analogous palladium clusters,[1] for which obviously this coupling does not exist, a similar conclusion holds.

However, another mechanism that was mentioned for these clusters[1] could also account for the present observations. It consists of a rapid "opening" (on the NMR time scale) of the core structure

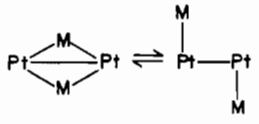

whereby rapid CO exchange could easily take place in the "open" form.

Experimental Section

A. Reagents and Physical Measurements. All reactions were performed in Schlenk-type flasks under nitrogen or argon if specified. Solvents were distilled under argon from sodium benzophenone–ketyl prior to use, except for dichloromethane, which was dried and distilled from P_2O_5. Ethanol was distilled from $Mg(OEt)_2$. Nitrogen (Air Liquide purified grade) was passed through a BASF R3-11 catalyst and molecular sieve columns to remove residual oxygen and water.

Column chromatography was performed under nitrogen with silica gel (Kieselgel 60, Merck) or Celite (545, Prolabo).

(40) Bodner, G. M.; Todd, L. J. *Inorg. Chem.* **1974**, *13*, 1335.
(41) Darensbourg, M. Y.; Jimenez, P.; Sackett, J. R.; Hanckel, J. M.; Kump, R. L. *J. Am. Chem. Soc.* **1982**, *104*, 1521.

Table V. Characterization of the Trimetallic Linear Complexes Ptm_2L_2

complex	color	mp, °C	formula (mol wt)	anal. calcd (found) % C	% H	% N
1a[a]	red-brown	>100 dec	$C_{30}H_{20}Cr_2N_2O_6Pt$ (803.58)	44.84 (44.60)	2.50 (2.39)	3.48 (3.40)
1b[a]	red	170 dec	$C_{26}H_{28}Cr_2N_2O_6Pt$ (763.60)	40.90 (40.60)	3.70 (3.68)	3.67 (3.64)
1c	red	198	$C_{30}H_{32}Cr_2N_2O_6Pt$ (815.67)	44.17 (44.21)	3.95 (3.93)	3.43 (3.58)
2a[a]	red	>130 dec	$C_{30}H_{20}Mo_2N_2O_6Pt$ (891.47)	40.41 (40.40)	2.26 (2.17)	3.14 (3.33)
3a[a]	orange	>130 dec	$C_{30}H_{20}N_2O_6PtW_2$ (1067.29)	33.76 (33.83)	1.88 (2.05)	2.62 (2.73)
4a	orange-brown	>90 dec	$C_{24}H_{10}Mn_2N_2O_6Pt$ (791.32)	36.43 (36.40)	1.27 (1.40)	3.54 (3.45)
4d	claret	78 dec	$C_{12}Mn_2O_{12}Pt$ (641.01)	22.49 (22.30)		

[a] This complex is light sensitive.

Table VIII. Characterization of the Clusters $Pt_2M_2Cp_2(CO)_6(PR_3)_2$

complex	color	mp, °C	formula (mol wt)	anal. calcd (found) % C	% H
5f	red-violet	>200	$C_{28}H_{40}Cr_2O_6P_2Pt_2$ (1028.74)	32.69 (32.60)	3.92 (3.87)
5g[a]	violet	b	$C_{40}H_{64}Cr_2O_6P_2Pt_2$ (1197.06)		
5h	green	>200	$C_{52}H_{40}Cr_2O_6P_2Pt_2$ (1353.29)	46.15 (46.25)	5.66 (5.49)
6e	violet	>200	$C_{22}H_{28}Mo_2O_6P_2Pt_2$ (1032.47)	25.59 (25.35)	2.73 (2.62)
6f	violet	>200	$C_{28}H_{40}Mo_2O_6P_2Pt_2$(1116.63)	30.12 (29.98)	3.61 (3.4)
6g	red-brown	b	$C_{40}H_{64}Mo_2O_6P_2Pt_2$ (1284.95)	37.4 (37.1)	5.02 (5.13)
6h	brown	>200	$C_{52}H_{40}Mo_2O_6P_2Pt_2$ (1404.89)	44.46 (44.48)	2.87 (2.92)
7e	brown	>200	$C_{22}H_{28}O_6P_2Pt_2W_2$ (1208.29)	21.87 (21.70)	2.34 (2.25)
7f	brown	>200	$C_{28}H_{40}O_6P_2Pt_2W_2$ (1292.45)	26.02 (26.12)	3.12 (2.99)
7g	brown	b	$C_{40}H_{64}O_6P_2Pt_2W_2$ (1460.77)	32.89 (32.5)	4.41 (4.29)
7h	brown	>200	$C_{52}H_{40}O_6P_2Pt_2W_2$ (1580.72)	39.51 (39.47)	2.55 (2.50)

[a] 5g is unstable and has only been characterized by IR spectroscopy. [b] The mp could not be determined with accuracy.

Elemental analyses of C, H, N, and P were performed by the Service Central de Microanalyses du CNRS.

Infrared spectra were recorded in the region 4000–400 cm^{-1} on a Perkin-Elmer 398 spectrophotometer as KBr pellets and Nujol mulls and in the region 420–50 cm^{-1} on a Polytec FIR 30 FT interferometer as polythene disks.

The ^1H, $^{13}C\{^1H\}$, and $^{31}P\{^1H\}$ NMR spectra were recorded at 90.00, 200.13, or 250.00; 22.63, 50.32, or 62.86; and 36.43 MHz, respectively, on a FT Brucker WH-90, Brucker WP 200SY, or Cameca 250 instrument. Proton and carbon chemical shifts are positive downfield relative to external Me_4Si. Positive phosphorus chemical shifts indicate a downfield position relative to H_3PO_4.

B. Synthesis. The phosphine ligands PEt_3, P-*n*-Bu_3, and PPh_3 were used as received (Fluka commercial grade), except PMe_3, which was prepared according to the procedure described in the literature[42] (Me = CH_3; Et = C_2H_5; Bu = C_4H_9; Ph = C_6H_5).

The platinum complexes *cis*- or *trans*-$PtCl_2L_2$ were prepared according to the literature methods for L = PhCN,[43] *t*-BuNC,[8] c-$C_6H_{11}NC$,[8] PEt_3,[43] and PPh_3.[43]

The sodium carbonylmetalates $Na[M(CO)_3Cp]$ (M = Cr, Mo, W) were prepared according to the literature[20,44-47] and our modifications.[1]

$Na[Mn(CO)_5]$ was obtained by Na/Hg[48] reduction of $Mn_2(CO)_{10}$ (Alfa Ventron commercial grade). CO was purchased from Air Liquide (B 20).

The reactions described below were monitored by IR spectroscopy in the ν(CO) region.

Linear Trimetallic Complexes. A typical experiment is detailed below for **1a**; the quantitative data for the analogous syntheses are given in Table IV, supplementary material. Infrared data for these complexes are given in Table I, and their characterization is presented in Table V.

Preparations. ***trans*-Pt[Cr(CO)$_3$Cp]$_2$(PhCN)$_2$ (1a).** Solid Na[Cr(CO)$_3$Cp]-2DME (10.11 g, 25 mmol) was slowly added at −40 °C to a stirred suspension of $PtCl_2(PhCN)_2$ (5.90 g, 12.5 mmol) in THF (160 mL). Under constant agitation the temperature was slowly raised to reach 20 °C in 8 h.

The resulting red-brown mixture was filtered. The solid was dried, washed with water (to remove NaCl) and EtOH, and dried in vacuo to give a red-brown powder of **1a**, 7.50 g (9.33 mmol, 75% based on Pt). More product contained in the dark red-brown THF filtrate was not further collected (decomposition).

***trans*-Pt[Mn(CO)$_5$]$_2$(CO)$_2$ (4d).** **4a** (0.50 g, 0.63 mmol) was dissolved in toluene (100 mL), and carbon monoxide was slowly bubbled into the solution for 6 h. The resulting mixture was evaporated

(42) Markam, R. T.; Dietz, E. A.; Martin, D. R. *Inorg. Synth.* **1976**, *16*, 153.
(43) Hartley, F. R. *Organomet. Chem. Rev., Sect. A* **1970**, *6*, 119.
(44) Hayter, R. G. *Inorg. Chem.* **1963**, *2*, 1031.
(45) Piper, T. S.; Wilkinson, G. *J. Inorg. Nucl. Chem.* **1956**, *3*, 104.
(46) Birdwhistell, R.; Hackett, P.; Manning, A. R. *J. Organomet. Chem.* **1978**, *157*, 239.
(47) Fischer, E. O.; Hafner, W.; Stahl, H. O. *Z. Anorg. Allg. Chem.* **1955**, *282*, 47.
(48) Hieber, W.; Wagner, G. *Z. Naturforsch., B: Anorg. Chem., Org. Chem., Biochem., Biophys., Biol.* **1958**, *13B*, 339.

to dryness, and the residue was washed with pentane and dried in vacuo, affording **4d** as a claret powder, 0.36 g (0.57 mmol, 90% based on Pt).

Cluster Syntheses. Two different synthetic methods have been developed and are discussed in the text. The first, method A, involves the reaction of the sodium carbonylmetalates with the $PtCl_2(PR_3)_2$ complexes, whereas method B concerns the reaction of free PR_3 with the isolated linear trimetallic complexes *trans*-$Pt[M(CO)_3Cp]_2(PhCN)_2$ formed from $PtCl_2(PhCN)_2$. Detailed syntheses of complexes **5f**, **6f**, and **7f** are given below. The others are summarized in Tables VI (method A) and VII (method B), supplementary material. Infrared and NMR data (where available) are given in Tables II and III, respectively. The characterization of all the Pt_2M_2 clusters is presented in Table VIII.

$Pt_2Cr_2Cp_2(CO)_6(PEt_3)_2$ (5f). Method A. A filtered solution of $Na[Cr(CO)_3Cp]$ (6 mmol) in THF (75 mL) prepared by Na/Hg reduction of $[Cr(CO)_3Cp]_2$ (1.21 g, 3 mmol) was added at room temperature to a stirred suspension of *trans*-$PtCl_2(PEt_3)_2$ (1.51 g, 3 mmol) in THF (25 mL). After 5 h of stirring, the dark green solution was filtered and the solvent was removed in vacuo. The residue was chromatographed on a silica gel column. Elution with toluene/pentane (4:15) gave a green solution of $[Cr(CO)_3Cp]_2$, 0.13 g (0.33 mmol, 11% based on Cr after recrystallization from toluene/pentane at −15 °C). Further elution with toluene/pentane (1:1) afforded $[Cr(CO)_2Cp]_2$, 0.05 g (0.15 mmol, 5% based on Cr), characterized by IR spectroscopy and elemental analysis. IR (KBr): ν(CO) 1900 s, 1880 s cm^{-1}. Anal. Calcd for $C_{14}H_{10}Cr_2O_4$ (mol wt 346.22): C, 48.57; H, 2.91. Found: C, 48.45; H, 2.80. These values are in agreement with those reported by Wrighton et al.[20]

Using toluene as eluent produced an orange red solution of $Pt_5(CO)_6(PEt_3)_4$, 0.24 g (0.15 mmol, 25% based on Pt after recrystallization from CH_2Cl_2/pentane), characterized by IR, spectroscopy and elemental analysis.[18]

Elution with THF/toluene (2:10) gave a mixture of three compounds that have been separated by THF/pentane recrystallizations: $Pt_5(CO)_6(PEt_3)_4$ (traces); *trans*-$PtHCl(PEt_3)_2$ (0.02 g (0.05 mmol, 1.6% based on Pt); ν(PtH) = 2185 cm^{-1});[23] **5f** (0.05 g (0.05 mmol, 3.2% based on Pt after recrystallization from CH_2Cl_2/pentane)). Elution with THF afforded a trace amount of an unstable green compound that has not yet been identified. IR (KBr): ν(CO) 1822 s, 1773 s cm^{-1}.

Method B. PEt_3 (1.13 mmol) in THF (25 mL) was added dropwise at −76 °C to a stirred suspension of **1a** (0.91 g, 1.13 mmol) in THF (50 mL). The reaction was completed after 3 h of stirring and refluxing. The resulting dark red-brown mixture was evaporated to dryness, and the residue was chromatographed on a Celite column. Elution with toluene/pentane (2:10) afforded a red solution of $Pt_5(CO)_6(PEt_3)_4$,[18] 0.20 g (0.12 mmol, 55% based on Pt after recrystallization from CH_2Cl_2/pentane at −15 °C). Further elution with toluene/pentane (3:10) gave a red-violet solution of **5f**, 0.03 g (0.03 mmol, 5.3% based on Pt after recrystallization from CH_2Cl_2/pentane at −15 °C). Using toluene as eluent produced a green unstable compound (trace amount) that has not yet been identified (see also method A). IR (KBr): ν(CO) 1822 vs, 1773 vs cm^{-1}.

$Pt_2Mo_2Cp_2(CO)_6(PEt_3)_2$ (6f). Method A. A filtered solution of $Na[Mo(CO)_3Cp]$ (8 mmol) in THF (50 mL) prepared by Na/Hg reduction of $[Mo(CO)_3Cp]_2$ (1.92 g, 4 mmol) was added at room temperature to a stirred suspension of *cis*-$PtCl_2(PEt_3)_2$ (2.01 g, 4 mmol) in THF (10 mL). After 2 h of stirring, the mixture was filtered and the solvent was removed in vacuo. The residue was chromatographed on a silica gel column. Elution with a toluene/pentane mixture (1:1) gave a red solution of $[Mo(CO)_3Cp]_2$ (trace amount). Further elution with toluene/pentane (2:1) afforded a red solution of $Pt_5(CO)_6(PEt_3)_4$, 0.05 g (0.03 mmol, 3.8% based on Pt after recrystallization from CH_2Cl_2/pentane).[18] Using THF/toluene (15:100) as eluent produced a dark red-brown solution of **6f**, 1.00 g (0.9 mmol, 45% based on Pt after recrystallization from THF/pentane).

Method B. PEt_3 (0.21 g, 1.78 mmol) in THF (20 mL) was added dropwise at room temperature to a stirred suspension of **2a** (1.59 g, 1.78 mmol) in THF (50 mL). The reaction was completed after 3 h of stirring and refluxing. The resulting red-brown mixture was evaporated to dryness, and the residue was chromatographed on a Celite column. Elution with toluene/pentane (1:1) afforded a red solution of $[Mo(CO)_3Cp]_2$, 0.33 g (0.67 mmol, 37.6% based on Mo after recrystallization from toluene/pentane at −15 °C). Further elution with toluene/pentane (2:1) gave a red solution of $Pt_5(CO)_6(PEt_3)_4$, 0.25 g (0.16 mmol, 45% based on Pt after recrystallization from CH_2Cl_2/pentane).[18] Using toluene as eluent produced a red-brown solution of **6f**, 0.49 g (0.44 mmol, 49.3% based on Pt after recrystallization from CH_2Cl_2/pentane).

$Pt_2W_2Cp_2(CO)_6(PEt_3)_2$ (7f). Method A. A filtered solution of $Na[W(CO)_3Cp]$ in THF (100 mL) (14 mmol) prepared by Na/Hg reduction of $[W(CO)_3Cp]_2$ (4.66 g, 7 mmol) was added at room temperature to a stirred suspension of *trans*-$PtCl_2(PEt_3)_2$ (3.51 g, 7 mmol) in THF (30 mL). After 5 h of stirring, the mixture was filtered and the solvent was removed in vacuo. The residue was chromatographed on a silica gel column. Elution with toluene/pentane (1:1) gave a red solution of $[W(CO)_3Cp]_2$, 1.90 g (2.85 mmol, 41% based on W), and $Pt_5(CO)_6(PEt_3)_4$, 0.02 g (0.01 mmol, 0.6% based on Pt).[18] Further elution with THF/toluene (2:1) afforded a red-brown solution of **7f**, 1.50 g (1.16 mmol, 33% based on Pt).

Method B. PEt_3 (0.145 g, 1.23 mmol) in THF (25 mL) was added dropwise at 0 °C to a stirred suspension of **3a** (1.31 g, 1.23 mmol) in THF (50 mL). Under constant agitation the temperature was slowly raised to reach 20 °C in 3 h and maintained at 20 °C for 3 h. The resulting red-brown mixture was evaporated to dryness, and the residue was chromatographed on a Celite column. Elution with toluene/pentane (1:2) gave a red solution of $[W(CO)_3Cp]_2$, 0.35 g (0.52 mmol, 43% based on W), and $Pt_5(CO)_6(PEt_3)_4$, 0.23 g (0.14 mmol, 57% based on Pt).[18] Further elution with toluene afforded a red-brown solution of **7f**, 0.26 g (0.2 mmol, 33% based on Pt after recrystallization from CH_2Cl_2/pentane).

Reaction of 4a with PPh_3: Obtention of $Pt_5(CO)_6(PPh_3)_4$. The two synthetic methods used above were unsuccessful in the case of Mn for obtaining mixed-metal clusters.[36b] Method A has previously been shown to afford an homopentametallic platinum cluster.[18] Method B has given the following results:

Under N_2: PPh_3 (0.66 g, 2.52 mmol) in THF (25 mL) was added dropwise at room temperature to a stirred suspension of **4a** (2.5 g, 3.16 mmol) in THF (50 mL). The reaction was completed after 3 h of stirring and refluxing. The resulting orange mixture was evaporated to dryness. The residue was washed with hexane, affording a red powder of $Pt_5(CO)_6(PPh_3)_4$, 0.97 g (0.44 mmol, 70% based on Pt after recrystallization from CH_2Cl_2/hexane).[18] The hexane solution and the CH_2Cl_2/hexane filtrate produced $Mn_2(CO)_{10}$, 0.74 g (1.90 mmol, 60% based on Mn). Anal. Calcd for $C_{78}H_{60}O_6P_4Pt_5$ (mol wt 2193): C, 42.73; H, 2.76. Found: C, 42.6; H, 2.9.

Under CO: PPh_3 (1.325 g, 5.05 mmol) in THF (50 mL) was added dropwise at room temperature to a stirred solution of **4a** (5 g, 6.32 mmol) in THF (50 mL). After 5.3 h of stirring at room temperature, the dark red mixture was concentrated to 100 mL and filtered, affording a red solid A (1.36 g) and a orange-red solution B. Solid A produced after washing with THF (200 mL) a brown violet powder of $[Pt(CO)PPh_3]_n$, 0.33 g (11% based on Pt), characterized by IR specroscopy and elemental analysis (see Discussion). IR (KBr): ν(CO) 1800 vs, cm^{-1}.[36a] Anal. Calcd for $C_{19}H_{15}OPPt$: C, 47.01; H, 3.11; P, 6.38; Pt, 40.19. Found: C, 46.92; H, 2.90; P, 6.70; Pt, 40.60. The THF filtrate gave **4d**, 1 g (1.56 mmol, 25% based on Pt), after precipitation with pentane. Solution B afforded $Pt_5(CO)_6(PPh_3)_4$, 1.26 g (0.58 mmol, 46% based on Pt), after addition of pentane and filtration. The THF/pentane filtrate gave $Mn_2(CO)_{10}$, 1.05 g (2.69 mmol, 42.6% based on Mn), after evaporation and recrystallization from hexane at −30 °C.

C. Collection of X-ray Data and Structure Determination. Single crystals of **5f**, **6f**, and **7f** were obtained by slow diffusion of pentane into a THF solution of the complexes. Cell constants and other pertinent data are presented in Tables IX and X. Intensity data were collected on a four-circle Nonius CAD 4 diffractometer. No intensity decay was observed during the data collection periods. The quality of the structure determination is given by R (Tables IX and X) and the σ values (Tables XVI and XVII). Absorption corrections were not performed. The structures were solved by Patterson and Fourier methods. Refinements by full-matrix least squares (all non-hydrogen atoms anisotropic) have proceeded to the R factor values indicated in Tables IX and X, using the SHELX[49] method for **5f** and the Busing ORX FLS 3 method[50] for **6f** and **7f**. Final positional and thermal

(49) Sheldrick, G. M. "ShelX Crystallographic Calculation Program"; University of Göttingen: Göttingen, West Germany.
(50) Busing, W. R.; Martin, K. O.; Levy, M. A.; Ellison, R. D.; Hamilton, W. C.; Ibers, J. A.; Johnson, C. K.; Thiessen, W. E. "ORX FLS 3"; Oak Ridge National Laboratory: Oak Ridge, TN, 1971.

Table IX. Summary of Crystal Data and Intensity Collection of **5f** and **6f**

compd	$Pt_2Cr_2Cp_2(CO)_6(PEt_3)_2$ (**5f**)	$Pt_2Mo_2Cp_2(CO)_6(PEt_3)_2$ (**6f**)
formula	$C_{28}H_{40}Cr_2O_6P_2Pt_2$	$C_{28}H_{40}Mo_2O_6P_2Pt_2$
fw	1028.74	1116.63
cryst syst	monoclinic	triclinic
a, Å	10.765 (6)	10.026 (2)
b, Å	9.430 (4)	11.155 (4)
c, Å	17.450 (5)	15.126 (4)
α, deg	90	85.17 (2)
β, deg	115.37 (2)	75.44 (2)
γ, deg	90	84.33 (2)
V, Å^3	1600.6	1618.8
Z	2	2
ρ(calcd), g cm^{-3}	2.13	2.29
cryst dimens, sphere ϕ, mm	8×10^{-2}	8×10^{-2}
space group	$P2_1/c$	$P\bar{1}$
temp, °C	25	25
radiation	Mo Kα (from monochromator, λ(Mo Kα_1) = 0.709 30 Å)	Mo Kα
linear abs coeff, cm^{-1}	99.6	99.3
μr (av)	0.82	0.87
scan θ/scan ω	1/1	2/3
scan width, deg	1 + 0.35 tan θ	1.5 + 0.35 tan θ
θ limits, deg	1.50–30	1–27
no. of data collcd ($I \geq 3\sigma(I)$)	4472	7326
no. of unique data used	2321	4574
$R = \Sigma\|\|F_o\| - \|F_c\|\|/\Sigma\|F_o\|$	0.032	0.051

Table X. Summary of Crystal Data and Intensity Collection of **7f**

compd	$Pt_2W_2Cp_2(CO)_6(PEt_3)_2$ (**7f** A)	$Pt_2W_2Cp_2(CO)_6(PEt_3)_2$ (**7f** B)
formula	$C_{28}H_{40}W_2O_6P_2Pt_2$	$C_{28}H_{40}W_2O_6P_2Pt_2$
fw	1292.45	1292.45
cryst syst	monoclinic	monoclinic
a, Å	8.768 (7)	11.920 (2)
b, Å	14.147 (2)	12.930 (6)
c, Å	13.580 (6)	12.166 (3)
β, deg	77.96 (5)	61.72 (2)
V, Å^3	1647.0	1651
Z	2	2
ρ(calcd), g cm^{-3}	2.60	2.60
cryst dimens, sphere ϕ, mm	6×10^{-2}	8×10^{-2}
space group	$P2_1/n$	$P2_1/n$
temp, °C	25	25
radiation	Mo Kα (from monochromator, λ(Mo Kα_1) = 0.709 30 Å)	Mo Kα
linear abs coeff, cm^{-1}	160	160
μr (av)	1.01	1.28
scan θ/scan ω	1/1	1/1
scan width, deg	1 + 0.35 tan θ	1 + 0.35 tan θ
θ limits, deg	1.50–27	1.50–27
no. of data collcd ($I \geq 3\sigma(I)$)	4188	4262
no. of unique data used	2365	1921
$R = \Sigma\|\|F_o\| - \|F_c\|\|/\Sigma\|F_o\|$	0.033	0.085

parameters (B_{eq}) for the three complexes are given in Tables XI–XV. Anisotropic thermal parameters and observed and calculated structure factor amplitudes of the reflections used in the refinement of all four structures are available as supplementary material.[51]

Table XI. Atomic Coordinates (×10^4) and Equivalent Thermal Parameters[a] for $Pt_2Cr_2Cp_2(CO)_6(PEt_3)_2$ (**5f**)

atom[b]	x/a	y/b	z/c	B_{eq}, Å^2
Pt	801 (1)	5700 (1)	4745 (1)	2.22 (2)
Cr	1817 (2)	3372 (2)	5772 (1)	2.42 (1)
P	2147 (3)	7004 (3)	4284 (2)	2.7 (1)
O(1)	−360 (9)	1472 (8)	4554 (5)	4.5 (4)
O(2)	1381 (9)	5943 (8)	6673 (5)	4.8 (4)
O(3)	2527 (11)	3568 (8)	4313 (6)	4.3 (5)
C(1)	306 (11)	2334 (11)	5030 (6)	3.5 (6)
C(2)	1302 (12)	5068 (13)	6189 (7)	4.2 (5)
C(3)	2115 (13)	3789 (12)	4824 (8)	5.7 (6)
C(4)	3536 (15)	3409 (16)	7040 (8)	4.1 (4)
C(5)	2605 (14)	2366 (19)	7025 (9)	5.1 (5)
C(6)	2525 (15)	1313 (14)	6417 (9)	4.2 (4)
C(7)	3428 (14)	1731 (13)	6055 (8)	5.3 (5)
C(8)	4044 (13)	3035 (16)	6445 (9)	5.1 (6)
C(9)	1752 (14)	8926 (11)	4159 (8)	5.3 (7)
C(10)	2716 (16)	9816 (14)	3900 (9)	6.5 (7)
C(11)	2101 (15)	6434 (13)	3260 (8)	5.6 (7)
C(12)	594 (16)	6389 (18)	2565 (8)	6.3 (8)
C(13)	3994 (12)	6893 (14)	4987 (8)	5.9 (7)
C(14)	4292 (15)	7382 (18)	5902 (8)	6.7 (8)

[a] Equivalent thermal parameter is in the form $B_{eq} = 4/3[\beta_{11}a^2 + \beta_{22}b^2 + \beta_{33}c^2 + 2\beta_{12}(ab\cos\gamma) + 2\beta_{13}(ac\cos\beta) + 2\beta_{23}(bc\cos\alpha)]$. [b] Atoms are labeled in agreement with Figure 2.

Table XII. Atomic Coordinates (×10^4) and Equivalent Thermal Parameters[a] for $Pt_2Mo_2Cp_2(CO)_6(PEt_3)_2$ (**6f** A)

atom[b]	x/a	y/b	z/c	B_{eq}, Å^2
Pt	−857 (1)	770 (1)	566 (1)	2.15 (2)
Mo	1929 (1)	1220 (1)	−15 (1)	2.49 (5)
P	−1990 (1)	2294 (4)	1468 (3)	2.6 (1)
O(1)	3655 (16)	50 (14)	−1773 (11)	4.6 (4)
O(2)	1047 (16)	−630 (14)	1702 (10)	4.8 (5)
O(3)	9836 (14)	2802 (12)	−902 (10)	3.7 (4)
C(1)	2701 (21)	244 (17)	−1091 (14)	3.3 (5)
C(2)	1167 (22)	−8 (20)	1035 (16)	4.0 (6)
C(3)	444 (17)	2065 (16)	−518 (12)	2.7 (4)
C(4)	2627 (23)	2473 (20)	923 (16)	4.1 (6)
C(5)	2562 (21)	3135 (18)	71 (16)	3.8 (6)
C(6)	3559 (22)	2587 (20)	−660 (17)	4.3 (6)
C(7)	4273 (21)	1565 (20)	−283 (18)	4.3 (7)
C(8)	3687 (22)	1519 (20)	703 (17)	4.3 (7)
C(9)	−1068 (19)	3664 (16)	1327 (13)	2.9 (5)
C(10)	−1851 (22)	4744 (18)	1875 (15)	3.8 (6)
C(11)	7576 (25)	1928 (20)	2719 (14)	4.3 (6)
C(12)	8866 (28)	1515 (22)	3072 (17)	5.0 (8)
C(13)	6321 (20)	2862 (18)	1286 (15)	3.6 (6)
C(14)	6433 (25)	3421 (23)	295 (18)	5.1 (8)

[a] Equivalent thermal parameter is in the form $B_{eq} = 4/3[\beta_{11}a^2 + \beta_{22}b^2 + \beta_{33}c^2 + 2\beta_{12}(ab\cos\gamma) + 2\beta_{13}(ac\cos\beta) + 2\beta_{23}(bc\cos\alpha)]$. [b] Atoms are labeled in agreement with Figure 3.

Results and Discussion of the Crystal Structures

Selected bond distances and angles of $Pt_2M_2Cp_2(CO)_6(PEt_3)_2$ [M = Cr (**5f**), Mo (**6f**), W (**7f**)] are given in Tables XVI and XVII, respectively, and more complete data are available in the supplementary material (Tables XVIS and XVIIS). Selected least-squares planes are given in Table XVIII, supplementary material. The labeling scheme used in the description of these molecules on the ORTEP plots is given

(51) See paragraph at the end of paper regarding supplementary material.
(52) Yoshida, T.; Yamagata, T.; Tulip, T. H.; Ibers, J. A.; Otsuka, S. *J. Am. Chem. Soc.* **1978**, *100*, 2063.
(53) Skapski, A. C.; Troughton, P. G. H. *J. Chem. Soc. A* **1969**, 2772; *J. Chem. Soc., Chem. Commun.* **1969**, 170.
(54) Cheung, K. K.; Cross, R. J.; Forrest, K. P.; Wardle, R.; Mercer, M. *J. Chem. Soc., Chem. Commun.* **1971**, 875.
(55) Taylor, N. J.; Chieh, P. C.; Carty, A. J. *J. Chem. Soc., Chem. Commun.* **1975**, 448.
(56) Jans, J.; Naegeli, R.; Venanzi, L. M.; Albinati, A. *J. Organomet. Chem.* **1983**, *247*, C37.
(57) Wagner, K. P.; Hess, R. W.; Treichel, P. M.; Calabrese, J. C. *Inorg. Chem.* **1975**, *14*, 1121.
(58) Modinos, A.; Woodward, P. *J. Chem. Soc., Dalton Trans.* **1975**, 1516.
(59) Bender, R.; Braunstein, P.; Tiripicchio, A.; Tiripicchio-Camellini, M. *J. Chem. Soc., Chem. Commun.* **1984**, 42.
(60) Fischer, J.; Mitschler, A.; Weiss, R.; Dehand, J.; Nennig, J. F. *J. Organomet. Chem.* **1975**, *91*, C37.

Table XIII. Atomic Coordinates (×10⁴) and Equivalent Thermal Parameters[a] for $Pt_2Mo_2Cp_2(CO)_6(PEt_3)_2$ (**6f** B)

atom[b]	x/a	y/b	z/c	B_{eq}, Å²
Pt	−778 (1)	6021 (1)	4954 (1)	2.32 (2)
Mo	2005 (2)	5834 (1)	3837 (1)	2.57 (5)
P	7664 (5)	7650 (4)	4894 (3)	2.7 (1)
O(1)	825 (17)	8328 (14)	4524 (13)	5.6 (6)
O(2)	215 (17)	4095 (14)	3200 (11)	4.6 (5)
O(3)	2962 (15)	5414 (14)	5648 (10)	4.2 (4)
C(1)	950 (22)	7305 (19)	4386 (15)	3.8 (6)
C(2)	650 (21)	4635 (19)	3619 (13)	3.3 (5)
C(3)	2503 (18)	5492 (17)	5021 (13)	3.0 (5)
C(4)	3608 (34)	5225 (30)	2500 (22)	7.0 (10)
C(5)	4313 (24)	5678 (27)	3038 (19)	5.3 (8)
C(6)	3917 (28)	6911 (28)	3131 (18)	5.9 (9)
C(7)	2961 (28)	7210 (28)	2631 (21)	7.0 (9)
C(8)	2742 (29)	6098 (39)	2229 (18)	7.2 (11)
C(9)	5853 (20)	7264 (18)	5183 (15)	3.8 (6)
C(10)	4760 (24)	8322 (21)	5094 (17)	4.9 (7)
C(11)	7658 (24)	8890 (20)	5612 (16)	4.3 (7)
C(12)	7259 (35)	8567 (29)	6660 (19)	7.2 (11)
C(13)	7920 (24)	8410 (19)	3746 (14)	4.3 (6)
C(14)	7900 (28)	7523 (26)	3019 (17)	5.6 (8)

[a] Equivalent thermal parameter is in the form $B_{eq} = {}^4/_3[\beta_{11}a^2 + \beta_{22}b^2 + \beta_{33}c^2 + 2\beta_{12}(ab\cos\gamma) + 2\beta_{13}(ac\cos\beta) + 2\beta_{23}(bc\cos\alpha)]$. [b] Atoms are labeled in agreement with Figure 3.

Table XIV. Atomic Coordinates (×10⁴) and Equivalent Thermal Parameters[a] for $Pt_2W_2Cp_2(CO)_6(PEt_3)_2$ (**7f** A)

atom[b]	x/a	y/b	z/c	B_{eq}, Å²
Pt	268 (1)	926 (1)	14 (1)	2.41 (1)
W	1095 (1)	−245 (1)	1516 (1)	2.81 (1)
P	790 (4)	2500 (2)	−207 (2)	2.8 (1)
O(1)	460 (19)	1842 (8)	2036 (9)	7.1 (5)
O(2)	−3315 (12)	696 (9)	561 (8)	4.9 (3)
O(3)	2429 (12)	787 (7)	−2054 (7)	3.8 (3)
C(1)	667 (19)	1104 (10)	1585 (10)	3.9 (4)
C(2)	−2337 (18)	524 (11)	−84 (10)	3.8 (4)
C(3)	1123 (14)	592 (9)	−1692 (8)	4.5 (3)
C(4)	3416 (21)	−471 (15)	2086 (14)	5.6 (6)
C(5)	2564 (21)	−1330 (14)	2221 (13)	5.4 (5)
C(6)	1122 (21)	−1169 (14)	2906 (12)	5.4 (6)
C(7)	1040 (21)	−210 (15)	3222 (11)	5.4 (6)
C(8)	2527 (25)	232 (15)	2698 (14)	6.3 (6)
C(9)	2660 (19)	2840 (11)	80 (11)	4.2 (4)
C(10)	4028 (20)	2289 (15)	−433 (16)	6.4 (6)
C(11)	913 (18)	2901 (10)	−1509 (10)	3.8 (4)
C(12)	1348 (23)	3954 (12)	−1720 (13)	5.6 (5)
C(13)	−515 (20)	3337 (11)	509 (13)	4.9 (5)
C(14)	−2186 (24)	3274 (16)	343 (17)	7.1 (7)

[a] Equivalent thermal parameter is in the form $B_{eq} = {}^4/_3[\beta_{11}a^2 + \beta_{22}b^2 + \beta_{33}c^2 + 2\beta_{12}(ab\cos\gamma) + 2\beta_{13}(ac\cos\beta) + 2\beta_{23}(bc\cos\alpha)]$. [b] Atoms are labeled in agreement with Figure 3.

Table XV. Atomic Coordinates (×10⁴) and Equivalent Thermal Parameters[a] for $Pt_2W_2Cp_2(CO)_6(PEt_3)_2$ (**7f** B)

atom[b]	x/a	y/b	z/c	B_{eq}, Å²
Pt	146 (1)	249 (1)	992 (1)	2.38 (4)
W	699 (1)	−1793 (1)	37 (1)	2.49 (4)
P	391 (11)	947 (8)	2584 (10)	2.8 (3)
O(1)	−353 (35)	1441 (23)	−2671 (30)	4 (1)
O(2)	−2844 (29)	347 (27)	1928 (31)	5 (1)
O(3)	2188 (31)	1653 (37)	−706 (32)	6 (1)
C(1)	−461 (46)	1246 (35)	−1650 (46)	4 (1)
C(2)	−2023 (43)	844 (34)	1287 (40)	4 (1)
C(3)	1035 (52)	1392 (49)	−547 (56)	5 (1)
C(4)	−1341 (63)	3189 (37)	−795 (52)	5 (1)
C(5)	−2382 (51)	2845 (42)	254 (61)	5 (1)
C(6)	−1900 (61)	3114 (44)	1212 (46)	6 (1)
C(7)	−671 (57)	3465 (33)	627 (60)	5 (1)
C(8)	−373 (64)	3511 (58)	−558 (70)	7 (1)
C(9)	342 (45)	2358 (35)	2611 (45)	4 (1)
C(10)	557 (84)	2859 (54)	3732 (76)	8 (2)
C(11)	1858 (42)	511 (39)	2617 (42)	4 (1)
C(12)	3073 (59)	1018 (77)	1287 (79)	8 (2)
C(13)	−808 (54)	552 (43)	4173 (44)	5 (2)
C(14)	−2181 (49)	762 (48)	4507 (58)	5 (2)

[a] Equivalent thermal parameter is in the form $B_{eq} = {}^4/_3[\beta_{11}a^2 + \beta_{22}b^2 + \beta_{33}c^2 + 2\beta_{12}(ab\cos\gamma) + 2\beta_{13}(ac\cos\beta) + 2\beta_{23}(bc\cos\alpha)]$. [b] Atoms are labeled in agreement with Figure 3.

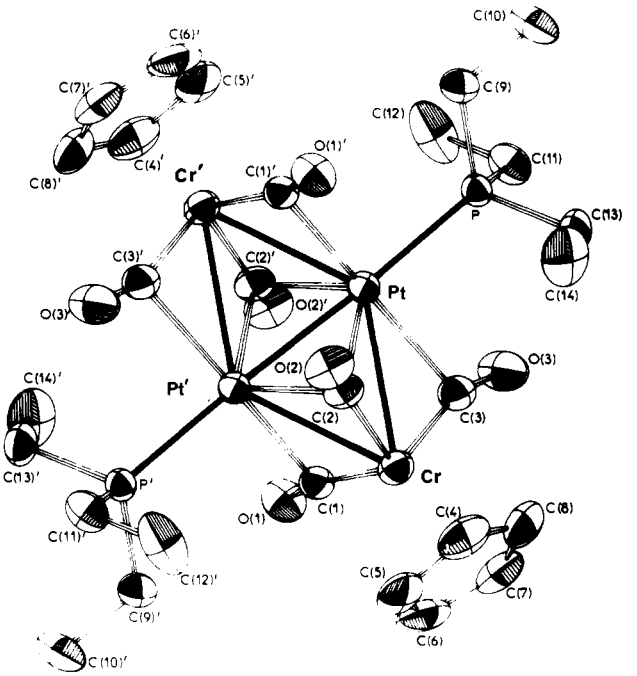

Figure 2. ORTEP diagram of the molecular structure of the $Pt_2Cr_2Cp_2(\mu_3\text{-}CO)_2(\mu\text{-}CO)_4(PEt_3)_2$ cluster (**5f**) illustrating the numbering scheme. Thermal ellipsoids enclose 50% of the electron density.

in Figures 2 and 3. In the case of complex **6f** (M = Mo) the asymmetric unit consists of two half-molecules. The unit cell contains two different centrosymmetric molecules called **6f** A B in the following, which are located on two independent inversion centers. Complex **7f** crystallizes in two different monoclinic cells, of $P2_1/n$ space group. These two types, called **7f** A B, have significantly different parameters along their binary axis (Table X). Both structures have been solved, that of molecule **7f** A leading to better *R* values (Table X).

The three molecules **5f**, **6f**, and **7f** have the same basic structure. Only the positions of the CO ligands differ slightly between **5f** (molecular structure in Figure 2) and **6f** and **7f** (molecular structure in Figure 3). The four metal atoms form a triangulated parallelogram with the center of symmetry at the middle of the Pt–Pt bond. Each of the two PEt_3 ligands is bonded to a Pt atom and is almost collinear with the Pt–Pt bond (170–178°; Table XVII). Each Cp ligand is η^5 bonded to an M atom whereas the CO ligands of each $M(CO)_3$ tripod occupy asymmetric bridging positions, with C(1)O(1) and C(3)O(3) between M and Pt′ or Pt, respectively, and C(2)O(2) between M, Pt, and Pt′. This arrangement was also found in the corresponding Pd_2M_2 clusters.[1] Because of the symmetry of these clusters, we shall only describe the arrangement of the carbonyl ligands on the MPtPt′ side.

Bond lengths and angles not involving the metal atom M are, in general, not significantly different (within 3σ) (Tables XVIS and XVIIS[51]) and will therefore often be quoted as average values in the following.

Metallic Core. We have discussed in the preceding paper dealing with the related $Pd_2M_2Cp_2(CO)_6L_2$ clusters[1] the originality and relevance of such heterometallic planar cores as models for multisite ligand–metal interactions.

The Pt–Pt′ distances range from 2.612 (1) (in **5f**) to 2.677 (2) Å (in **6f** A). These distances are rather short, as seen by comparison with literature data concerning selected Pt–Pt

Table XVI. Bond Lengths (Å) in Crystalline $Pt_2M_2Cp_2(CO)_6(PEt_3)_2$ Complexes (M = Cr, Mo, W)[a]

	compd				
		M = Mo (**6f**)		M = W (**7f**)	
bond[b]	M = Cr (**5f**)	A	B	A	B
Pt–Pt′	2.612 (1)	2.677 (1)	2.646 (1)	2.662 (1)	2.675 (2)
Pt–M	2.748 (1)	2.777 (2)	2.793 (1)	2.775 (1)	2.787 (2)
Pt′–M	2.709 (1)	2.835 (2)	2.846 (1)	2.836 (1)	2.833 (2)
Pt–P	2.292 (3)	2.284 (5)	2.289 (5)	2.281 (3)	2.28 (1)
Pt–C(1)	3.30 (1)	3.79 (2)	3.76 (2)	3.79 (1)	3.83 (6)
Pt–C(2)	2.42 (1)	2.38 (2)	2.25 (2)	2.38 (1)	2.56 (6)
Pt–C(3)	2.26 (1)	2.30 (1)	2.52 (2)	2.33 (1)	2.22 (6)
Pt′–C(1)	2.33 (1)	2.19 (2)	2.29 (2)	2.25 (1)	2.19 (5)
Pt′–C(2)	2.27 (1)	2.74 (3)	2.65 (2)	2.75 (1)	2.96 (4)
Pt′–C(3)	3.56 (1)	3.15 (2)	3.31 (2)	3.18 (1)	2.74 (4)
M–C(1)	1.86 (1)	1.97 (2)	1.98 (2)	1.94 (1)	1.97 (5)
M–C(2)	1.93 (2)	2.04 (2)	2.10 (2)	2.06 (1)	2.04 (4)
M–C(3)	1.86 (2)	1.97 (2)	1.98 (2)	1.97 (1)	1.93 (6)
C(1)–O(1)	1.16 (1)	1.22 (2)	1.16 (3)	1.20 (2)	1.21 (7)
C(2)–O(2)	1.16 (1)	1.16 (2)	1.10 (3)	1.12 (2)	1.13 (5)
C(3)–O(3)	1.17 (2)	1.18 (2)	1.15 (3)	1.18 (2)	1.36 (8)
M–C(Cp) (av)	2.20	2.34	2.33	2.32	2.30
M–centroid Cp	1.84 (1)	1.99 (1)	2.02 (1)	1.98 (1)	1.97 (1)
C–C (within Cp) (av)	1.41	1.43	1.39	1.43	1.42
P–$C(H_2)$ (av)	1.85	1.83	1.83	1.82	1.84
$C(H_2)$–$C(H_3)$ (av)	1.56	1.54	1.55	1.54	1.6

[a] Figures in parentheses are the estimated standard deviations in the last significant digit. [b] Atoms are labeled in agreement with Figure 2 (M = Cr) or Figure 3 (M = Mo, W).

Table XVII. Bond Angles (deg) in Crystalline $Pt_2M_2Cp_2(CO)_6(PEt_3)_2$ Complexes (M = Cr, Mo, W)[a]

	compd				
angle[b]	M = Cr (**5f**)	M = Mo (**6f** A)	M = Mo (**6f** B)	M = W (**7f** A)	M = W (**7f** B)
Pt′–Pt–M	60.7 (1)	62.60 (4)	63.05 (4)	62.83 (2)	62.45 (4)
M–Pt–M′	122.2 (1)	123.01 (4)	124.05 (3)	123.36 (2)	123.16 (4)
Pt–Pt′–M	61.5 (1)	60.41 (4)	61.00 (4)	60.53 (2)	60.71 (4)
Pt′–Pt–P	177.7 (1)	173.3 (1)	169.7 (1)	171.8 (2)	170.5 (3)
Pt–M–Pt′	57.2 (1)	56.99 (4)	55.95 (4)	56.63 (2)	56.85 (4)
C(1)–M–C(2)	112.9 (5)	105 (1)	114 (1)	107.0 (6)	105 (2)
C(1)–M–C(3)	85.7 (5)	94 (1)	86 (1)	93.6 (6)	88 (2)
C(2)–M–C(3)	110.3 (5)	112 (1)	111 (1)	112.4 (6)	113 (2)
Pt′–C(1)–M	83.1 (7)	85.7 (7)	83.1 (8)	84.8 (5)	86 (2)
Pt′–C(1)–O(1)	120.7 (7)	127 (2)	124 (2)	122 (1)	127 (3)
M–C(1)–O(1)	161.8 (9)	147 (2)	153 (2)	152 (1)	146 (4)
Pt–C(2)–Pt′	67.7 (7)	62.6 (6)	64.6 (5)	61.9 (8)	57 (2)
Pt–C(2)–M	77.5 (7)	77.2 (8)	79.6 (7)	76.1 (8)	73 (3)
Pt′–C(2)–M	79.9 (7)	71.1 (7)	72.4 (6)	71.3 (8)	66 (3)
Pt–C(2)–O(2)	119.9 (8)	119 (2)	121 (1)	119 (1)	115 (3)
Pt′–C(2)–O(2)	119.4 (8)	123 (2)	126 (1)	123 (1)	114 (3)
M–C(2)–O(2)	157.0 (9)	161 (2)	155 (2)	162 (1)	170 (5)
Pt–C(3)–M	83.1 (7)	80.6 (6)	75.5 (7)	79.9 (7)	84 (3)
Pt–C(3)–O(3)	122.6 (9)	117 (1)	115 (1)	117 (1)	110 (3)
M–C(3)–O(3)	155 (1)	161 (2)	169 (2)	163 (1)	150 (5)
C–M–C (adj C in Cp) (av)	37.5	36	35	35.9	35
C–C–C (adj C in Cp) (av)	108	108	108	108	108
Pt–P–$C(H_2)$ (av)	114.5	115.4	114.7	115.3	114
$C(H_2)$–P–$C(H_2)$ (av)	104.0	103	103	103	104
P–$C(H_2)$–$C(H_3)$ (av)	112.0	114	104	115	111

[a] Figures in parentheses are the estimated standard deviations in the last significant digit. [b] Atoms are labeled in agreement with Figure 2 (M = Cr) or Figure 3 (M = Mo, W).

distances and fall in the range found for Pt(I)–Pt(I) bonds (Table XIX).

In each of the four structures, the heterometallic Pt–M and Pt′–M distances are significantly different. The former are shorter in **6f** and **7f** whereas the opposite is found in **5f**. As discussed in the corresponding Pd_2M_2 clusters,[1] this can be related to the bonding modes of the carbonyl ligands. Thus, we find that when C(2)O(2) comes closer to Pt than to Pt′, which occurs when going from **5f** (M = Cr), with Pt–C(2) > Pt′–C(2), to **6f** (M = Mo) or **7f** (M = W) where Pt–C(2) < Pt′–C(2) (Figures 2 and 3), a shortening of the corresponding Pt–M distance is observed. Simultaneously, the Pt′–C(1) distance, which is longer than Pt–C(3) in **5f**, becomes shorter than Pt–C(3) in **6f** or **7f** (Table XVI). This is consistent with the fact that a shorter Pt–M distance is found where the contributions of the bridging carbonyls on this bond are higher.[1] This effect appears more pronounced in these clusters than in their palladium analogues,[1] as seen here by greater differences between the Pt–M and Pt–M′ distances, compared to the corresponding Pd–M and Pd–M′ distances. We can visualize the changes in the carbonyl to metal interactions from **5f** to **6f** or **7f** as resulting from a rotation of the $M(CO)_3$ tripod around the MM′ axis.

As seen in Table XX, where selected Pt–M (M = Cr, Mo, W) bond distances are given, the Pt_2M_2 clusters reported here were (M = Mo,[6] W[61]) or are (M = Cr) the first examples of

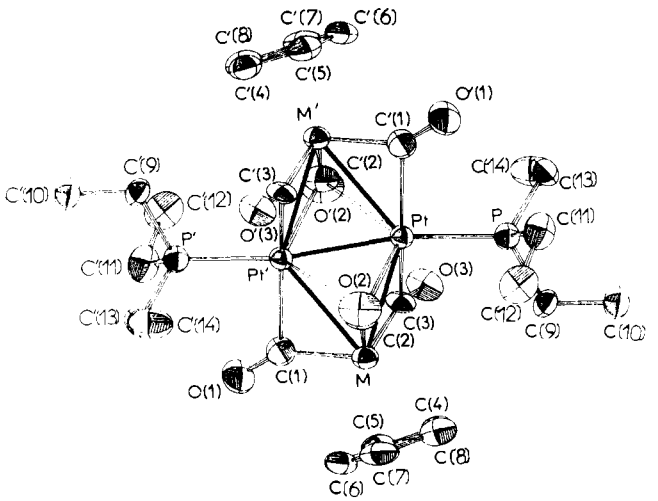

Figure 3. ORTEP diagram of the molecular structure of the $Pt_2M_2Cp_2(\mu_3\text{-}CO)_2(\mu\text{-}CO)_4(PEt_3)_2$ clusters (M = Mo (**6f**); W (**7f**)). Thermal ellipsoids enclose 50% of the electron density.

Table XIX. Selected Pt-Pt Bond Distances (Å)

complex[a]	Pt oxidn state	Pt-Pt dist	ref
metallic Pt	0	2.77	24
$Pt_2[(t\text{-}Bu)_2P(CH_2)_3P(t\text{-}Bu)_2]_2$	0	2.765 (1)[b]	52
$Pt_2(\mu\text{-}S)(CO)(PPh_3)_3$	1+	2.647 (2)	53
$Pt_2Cp_2(\eta^4\text{-}C_{10}H_{10})$	1+	2.581 (4)	54
$[Pt_2(\mu\text{-}PPh_2)_2(PPh_3)_2]\cdot C_6H_6$	1+	2.604 (1)	55
$[Pt_2(\mu\text{-}H)(\mu\text{-}PPh_2)(Ph)(PPh_3)_3]BF_4$		2.889 (2), 2.912 (2)	56
$Pt_2[\mu\text{-}\eta^2\text{-}SPEt_2]_2[P(OPh)_3]_2$	1+	2.628 (1)	57
$[Pt_2Cl_4(CO)_2][Pr_4N]_2$	1+	2.584 (2)[b]	58
$Pt_2Cl_2(\mu\text{-}CO)(PPh_3)_3\cdot 2C_6H_5Cl$	1+	2.643 (3)	59
$Pt_2Co(\mu\text{-}PPh_2)(CO)_3(PPh_3)_3$	1+	2.664 (1)	93
$Pt_2Cr_2Cp_2(\mu_3\text{-}CO)_2(\mu\text{-}CO)_4(PEt_3)_2$	1+	2.612 (1)	this work
$Pt_2Mo_2Cp_2(\mu_3\text{-}CO)_2(\mu\text{-}CO)_4(PEt_3)_2$	1+	2.677 (1), 2.646 (1)[c]	this work
$Pt_2W_2Cp_2(\mu_3\text{-}CO)_2(\mu\text{-}CO)_4(PEt_3)_2$	1+	2.662 (1), 2.675 (2)[c]	this work
$Pt_2Mn_2(\mu\text{-}PPh_2)_4(CO)_8$	1+	2.668 (1)	36b
$Pt_2Co_2(\mu\text{-}CO)_3(CO)_5(PPh_3)_2$	0	2.987 (4)[b]	60

[a] $Cp = \eta^5\text{-}C_5H_5$. [b] The Pt-Pt bond is not supported by a bridging ligand. [c] Value for the other molecule found in the solid state (see text).

platinum mixed-metal clusters with these metals to have been structurally characterized. To our knowledge, only few other Pt-W clusters have since been published.[74-78] As indicated in Table XX, only very few Pt-Cr or Pt-Mo distances have been reported so far.

The Pt-Cr, Pt-Mo, and Pt-W distances in **5f**, **6f**, and **7f** (Table XVI) are all much shorter than the sum of the corresponding covalent radii:[79] 2.95, 2.93, and 2.92 Å, respectively, when taking as covalent radius for M half the metal-metal distance in the corresponding $[M(CO)_3Cp]_2$ molecules (M = Cr,[80] 1.640 Å; M = Mo,[81] 1.617 Å; M = W,[81] 1.611 Å). These short metal-metal distances are related to the existence of the bridging carbonyls, producing a "flattening" of the $M(CO)_3$ tripod (see below).

Metal-Ligand Systems. The arrangement of the ligands in **5f** bears a stronger ressemblance than in **6f** and **7f** to that in the $Pd_2M_2Cp_2(CO)_6(PEt_3)_2$ clusters.[1] For example, the values of the Pt'-Pt-P angles (Table XVII) ranging from 169.7 to 173.3° for **6f** and **7f** are slightly different from that in **5f**, 177.7°, which in contrast compares well with the average value of 177° found for the Pd'-Pd-P angles in the Pd_2M_2 clusters. Deviations from linearity of the P-Pt-Pt'-P' array are probably due to steric effects (influence of the $M(CO)_3$ geometry) or packing forces. The Pt-P distances in these clusters (Table XVI) have an average value of 2.285 Å, intermediate between those found in *trans*-$HPtBr(PEt_3)_2$ (2.26 Å)[82] and *trans*-$PtBr_2(PEt_3)_2$ (2.315 Å).[83]

The planes of the η^5-cyclopentadienyl ligands form an angle of 75.6° (M = Cr), 86.9 or 77.5° (M = Mo), and 85.7 or 86° (M = W) with the plane of the four metals (Table XVIII[51]).

The $M(CO)_3Cp$ moieties present in these clusters bear a very strong structural analogy with those previously described in the corresponding Pd_2M_2 clusters.[1] The slight differences observed here in the carbonyl positions are related to the fact that Pt-M < Pt'-M in **6f** and **7f**, whereas Pt-M > Pt'-M in **5f**, as discussed above. Structural details for these fragments are given in Tables XVI-XVIII,[51] respectively.

Both the platinum-carbon (CO) distances, longer than for typical $Pt_2(\mu\text{-}CO)$ units,[18,84] and the M-C-O angles[1] support the description of C(1)O(1) and C(3)O(3) as semibridging and C(2)O(2) as semitriply bridging ligands.[85] This description is consistent with their ν(CO) stretching frequencies (vide supra).

The Pt_2 unit in these centrosymmetric molecules is located within the $M(CO)_3$ cone angle (Figures 2 and 3). Only in the analogous Pd_2M_2 clusters[1] have we found precedence for such a structural arrangement. Whereas a four-legged piano-stool structure is commonly found in the $M(CO)_3CpX$ molecules,[86]

(61) Braunstein, P.; Bender, R.; Dusausoy, Y.; Protas, J.; Ricard, L.; Fischer, J. IX International Conference on Organometallic Chemistry, Dijon, France, Sept, 1979; Abstract B64.
(62) Howard, J. A. K.; Jeffery, J. C.; Laguna, M.; Navarro, R.; Stone, F. G. A. *J. Chem. Soc., Dalton Trans.* **1981**, 751.
(63) Farr, J. P.; Olmstead, M. M.; Rutherford, N. M.; Wood, F. E.; Balch, A. L. *Organometallics* **1983**, *2*, 1758.
(64) Braunstein, P.; Keller, E.; Vahrenkamp, H. *J. Organomet. Chem.* **1979**, *165*, 233.
(65) Braunstein, P.; Jud, J. M.; Dusausoy, Y.; Fischer, J. *Organometallics* **1983**, *2*, 180.
(66) Ashworth, T. V.; Howard, J. A. K.; Laguna, M. *J. Chem. Soc., Dalton Trans.* **1980**, 1593.
(67) Howard, J. A. K.; Mead, K. A.; Moss, J. R.; Navarro, R.; Stone, F. G. A.; Woodward, P. *J. Chem. Soc., Dalton Trans.* **1981**, 743.
(68) Ashworth, T. V.; Howard, J. A. K.; Stone, F. G. A. *J. Chem. Soc., Chem. Commun.* **1979**, 42.
(69) Jeffery, J. C.; Moore, I.; Razay, H.; Stone, F. G. A. *J. Chem. Soc., Chem. Commun.* **1981**, 1255.
(70) Albinati, A.; Naegeli, R.; Togni, A.; Venanzi, L. M. *Organometallics* **1983**, *2*, 926.
(71) Mead, K. A.; Moore, I.; Stone, F. G. A.; Woodward, P. *J. Chem. Soc., Dalton Trans.* **1983**, 2083.
(72) Awang, M. R.; Jeffery, J. C.; Stone, F. G. A. *J. Chem. Soc., Dalton Trans.* **1983**, 2091.
(73) Jeffery, J. C.; Sambale, C.; Schmidt, M. F.; Stone, F. G. A. *Organometallics* **1982**, *1*, 1597.
(74) Chetcuti, M. J.; Howard, J. A. K.; Mills, R. M.; Stone, F. G. A.; Woodward, P. *J. Chem. Soc., Dalton Trans.* **1982**, 1757.
(75) Ashworth, T. V.; Chetcuti, M. J.; Howard, J. A. K.; Stone, F. G. A.; Wisbey, S. J.; Woodward, P. *J. Chem. Soc., Dalton Trans.* **1981**, 763.
(76) Ashworth, T. V.; Berry, M.; Howard, J. A. K.; Laguna, M.; Stone, F. G. A. *J. Chem. Soc., Chem. Commun.* **1979**, 45.
(77) Chetcuti, M. J.; Marsden, K.; Moore, I.; Stone, F. G. A.; Woodward, P. *J. Chem. Soc., Dalton Trans.* **1982**, 1749.
(78) Awang, M. R.; Carriedo, G. A.; Howard, J. A. K.; Mead, K. A.; Moore, I.; Nunn, C. M.; Stone, F. G. A. *J. Chem. Soc., Chem. Commun.* **1983**, 964.
(79) Pauling, L. "The Nature of the Chemical Bond", 3rd ed.; Cornell University Press: Ithaca, NY, 1960.
(80) Adams, R. D.; Collins, D. M.; Cotton, F. A. *J. Am. Chem. Soc.* **1974**, *96*, 749.
(81) Adams, R. D.; Collins, D. M.; Cotton, F. A. *Inorg. Chem.* **1974**, *13*, 1086.
(82) Owston, P. G.; Partridge, J. M.; Rowe, J. M. *Acta Crystallogr.* **1960**, *13*, 246.
(83) Messmer, G. G.; Amma, E. L. *Inorg. Chem.* **1966**, *5*, 1775.
(84) Albinati, A. *Inorg. Chim. Acta* **1977**, *22*, L31.
(85) Colton, R.; McCormick, M. J. *Coord. Chem. Rev.* **1980**, *31*, 1.
(86) Bueno, C.; Churchill, M. R. *Inorg. Chem.* **1981**, *20*, 2197.

Table XX. Heterobimetallic Pt-M Bond Distances (Å)

complex[a]	Pt-M dist	ref
Pt-Cr		
$PtCr[\mu\text{-}C(CO_2Me)Ph](CO)_4(PMe_3)_3$	2.646 (7)	62
$Pt_2Cr_2Cp_2(\mu_3\text{-}CO)_2(\mu\text{-}CO)_4(PEt_3)_2$	2.748 (1), 2.709 (1)	this work
Pt-Mo		
$PtMo(H)Cp(CO)_3(PPh_3)_2$	2.839 (1)[b]	13
$PtMo(\mu\text{-}Ph_2Ppy)_2(\mu\text{-}CO)(CO)_2Cl_2$	2.845 (1)	63
$[PtMoCp'(\mu\text{-dppm})(CO)_2(dppm)]_2Mo_2O_7$	2.912 (4)	95
trans-$Pt(C_6H_{11}NC)[C(OEt)NH(C_6H_{11})][Mo(CO)_3Cp]_2$	2.889 (2)[b]	64
$Pt_2Mo_2Cp_2(\mu_3\text{-}CO)_2(\mu\text{-}CO)_4(PEt_3)_2$	2.777 (2), 2.835 (2) 2.793 (1),[c] 2.846 (1)[c]	this work
$Pt_2Mo_2Cp_2(CO)_6(Ph_2PCH_2CH_2PPh_2)$	2.651 (4), 2.721 (2), 2.773 (3)	65
Pt-W		
$PtW[\mu\text{-}C(OMe)Ph](CO)_5(PMe_3)_2$	2.861 (1)	66
$PtW[\mu\text{-}C(OMe)C_6H_4Me\text{-}4](CO)_4(PMe_3)_3$	2.825 (1)	67
$PtWCp[\mu\text{-}CC_6H_4\text{-}p\text{-}Me](CO)_2(PMe_2Ph)_2$	2.753 (1)	68
$PtW(\mu\text{-}H)[\mu\text{-}CH(C_6H_4Me\text{-}4)]Cp(CO)_2(PMe_3)_2$	2.895 (1)	69
$[PtW[\mu\text{-}\eta^1,\eta^3\text{-}CH(C_6H_4Me\text{-}4)]Cp(CO)_2(PMe_3)_2][BF_4]$	2.795 (1)	69
$[PtW(\mu\text{-}H)_2(Ph)Cp_2(PEt_3)][BPh_4]$	2.663 (1)	70
$PtW[\mu\text{-}C(OMe)C_6H_4Me\text{-}4](CO)_5(\mu\text{-dppm})$	2.818 (3)	71
$PtW(\mu\text{-}C{=}CH_2)(CO)_5(dppm)$	2.774 (1)	72
$PtWCp[\mu\text{-}C(C_6H_4Me\text{-}4)C(O)](CO)(PMe_3)(\eta^4\text{-}C_8H_{12})$	2.728 (1)	73
$PtWFeCp(\mu_3\text{-}CC_6H_4Me\text{-}4)(CO)_6(PEt_3)$	2.775 (1)	74
$PtWFeCp(\mu_3\text{-}CC_6H_4Me\text{-}4)(CO)_5(PMePh_2)_2$	2.883 (1)	74
$PtW_2Cp_2(\mu\text{-}CC_6H_4Me\text{-}4)_2(CO)_4$	2.715 (1), 2.711 (1)	75
$Pt_2W[\mu\text{-}C(OMe)Ph](CO)_6(P\text{-}t\text{-}Bu_2Me)_2$	2.830 (2), 2.833 (2)	76
$Pt_2WCp(\mu_3\text{-}CC_6H_4Me\text{-}4)(CO)_4(PMePh_2)_2$	2.785 (3), 2.785 (3)	77
$Pt_2W_2Cp_2(\mu_3\text{-}CO)_2(\mu\text{-}CO)_4(PEt_3)_2$	2.775 (1), 2.836 (1) 2.787 (2),[c] 2.833 (2)[c]	this work
$Pt_2W_3Cp_3(\mu\text{-}CC_6H_4Me\text{-}4)_2(\mu_3\text{-}CC_6H_4Me\text{-}4)(CO)_6$	2.713 (2), 2.718 (2) 2.723 (2), 2.773 (2)	78
$Pt_3W_2Cp_2(\mu_3\text{-}CC_6H_4Me\text{-}4)_2(CO)_4(COD)_2$	2.748 (1), 2.751 (1)	78

[a] $Cp = \eta^5\text{-}C_5H_5$; $Cp' = \eta^5\text{-}C_5H_4Me$; dppm = $Ph_2PCH_2PPh_2$. [b] The Pt-M bond is not supported by a bridging ligand. [c] Value for the other molecule found in the solid state (see text).

the $M(CO)_3Cp$ fragment in these Pd_2M_2 clusters can be described as a three-legged piano stool bridging the Pt–Pt′ bond. The metal–metal separations are directly related to the flattening observed for the $M(CO)_3$ tripod (see Table XVII) when compared to the structure of the $M(CO)_3Cp^-$ anions. Thus, in $[Me_4N][Cr(CO)_3Cp]$, the average (O)C–Cr–C(O) angle is only 89.4°,[87] and in $Mo(CO)_3Cp^-$, the corresponding value was found to be 88.1° (for the $[(n\text{-}C_4H_9)_4N]^+$ salt[88]) or 86.3° (for the $[Cp_2Mo(H)CO]^+$ salt[89]).

Concerning the discriminating bonding modes of the CO ligands "preferring" M to Pt and their relevance as structural models for CO activation, we invite the reader to consult our paper on the related $Pd_2M_2Cp_2(CO)_6(PEt_3)_2$ clusters.[1] This will avoid redundancies.

Bonding Description. For the 58-electron $Pt_2M_2Cp_2(CO)_6(PR_3)_2$ clusters described in this work, the presence of two 18-electron group 6 metals M and of two 16-electron platinum atoms accounts for five metal–metal bonds. Diamagnetism is observed for these clusters between 298 and 4 K (Foner magnetometer). These molecules nicely illustrate the recently proposed cluster condensation generalization derived from molecular orbital calculations.[90]

From their synthetic origin, which indicates partial reduction of the Pt(II) precursor complexes, we envisage these clusters as formally containing two Pt(I) centers. This is further supported by the relatively short Pt–Pt distances (Table XIX). Similar considerations have been developed for the related Pd_2M_2 clusters.[1] We propose to formally consider the $[M(CO)_3Cp]^-$ fragments as 4-electron donors toward the $R_3P\rightarrow Pd(I)\text{–}Pd(I)\leftarrow PR_3$ or $R_3P\rightarrow Pt(I)\text{–}Pt(I)\leftarrow PR_3$ units. This results in a striking analogy between our clusters and the known complex $Pt_2(\mu\text{-}PPh_2)_2(PPh_3)_2$[55] in which the diphenylphosphido bridges behave as anionic 4-electron donors toward the Pt(I)–Pt(I) unit. This suggests an isolobal analogy[91] between the $\mu\text{-}PPh_2$ and the $\mu\text{-}[M(CO)_3Cp]$ fragments in these molecules:

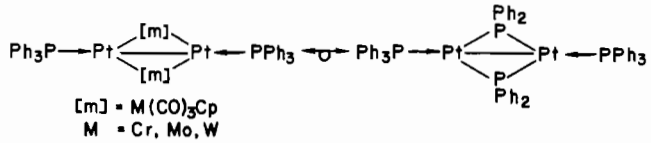

To what extent the electron donation occurs through the metal–metal bonds or through the carbonyl bridges cannot be stated presently. Electrochemical studies on the Pd_2M_2 and Pt_2M_2 clusters have been performed, and their results are consistent with the formalism proposed here.[92]

Moreover, we have recently shown that other carbonylmetalate fragments could behave in such an unusual way, as does $[Co(CO)_3PPh_3]^-$ in the $Pt_2Co(\mu\text{-}PPh_2)(\mu\text{-}CO)_2(CO)(PPh_3)_3$ cluster.[93] Finally, one example is now available with $\{[Pd(8\text{-mq})]_3[\mu_3\text{-}Mo(CO)_3Cp][\mu_3\text{-}Cl]\}BF_4$ where the $[Mo(CO)_3Cp]^-$ anion is symmetrically bonded to *three* metal atoms, behaving as a formal 6-electron donor.[94]

(87) Feld, R.; Hellner, E.; Klopsch, A.; Dehnicke, K. *Z. Anorg. Allg. Chem.* **1978**, *442*, 173.
(88) Crotty, D. E.; Corey, E. R.; Anderson, T. J.; Glick, M. D.; Oliver, J. P. *Inorg. Chem.* **1977**, *16*, 920.
(89) Adams, M. A.; Folting, K.; Huffman, J. C.; Caulton, K. G. *Inorg. Chem.* **1979**, *18*, 3020.
(90) Mingos, D. M. P.; Evans, D. G. *J. Organomet. Chem.* **1983**, 251, C13.
(91) Hoffmann, R. *Angew. Chem., Int. Ed. Engl.* **1982**, *21*, 711.
(92) Jund, R.; Lemoine, P.; Gross, M.; Bender, R.; Braunstein, P. *J. Chem. Soc., Chem. Commun.* **1983**, 86.
(93) Bender, R.; Braunstein, P.; Metz, B.; Lemoine, P. *Organometallics* **1984**, *3*, 381.
(94) Braunstein, P.; Fischer, J.; Matt, D.; Pfeffer, M. *J. Am. Chem. Soc.* **1984**, *106*, 410.

Conclusion

In this paper, we have described the syntheses, characterizations, and X-ray structures of a family of new heterotetrametallic Pt_2M_2 clusters, of general formula $Pt_2M_2Cp_2(CO)_6(PR_3)_2$ (M = Cr, Mo, W). When we began this work,[6,15] there was no platinum–group 6 mixed-metal cluster structurally characterized, despite the considerable interest for this area of inorganic chemistry.[3]

The X-ray structure determination of the three clusters $Pt_2M_2Cp_2(\mu_3\text{-}CO)_2(\mu\text{-}CO)_4(PEt_3)_2$ (M = Cr (**5f**); M = Mo (**6f**) with two different molecules A and B in the unit cell; M = W (**7f**) with two different unit cells, A and B) has revealed a planar, triangulated parallelogram framework for the metallic core, analogous to that found recently for the related $Pd_2M_2Cp_2(\mu_3\text{-}CO)_2(\mu\text{-}CO)_4(PEt_3)_2$ clusters.[1] The present structures possess a center of symmetry at the middle of the Pt–Pt′ bond. This distance is rather short, ranging from 2.612 (1) (in **5f**) to 2.677 (1) Å (in **6f** A). The heterometallic Pt–M distances have values of 2.748 (1) and 2.709 (1) Å for M = Cr, range from 2.777 (2) to 2.846 (1) Å for M = Mo, and range from 2.775 (1) to 2.836 (1) for M = W.

The difference between the Pt–M and the Pt′–M distances has been related to the bonding modes of the semibridging C(1)O(1) and C(3)O(3) and semitriply bridging C(2)O(2) carbonyl ligands. Thus, when μ_3-[C(2)O(2)] comes closer to Pt than to Pt′, which occurs when going from **5f** to **6f** or **7f** (Figures 2 and 3), a shortening of the corresponding Pt–M distance is observed. This parallels a shortening of the Pt′–C(1) distance relative to Pt–C(3) when going from **5f** to **6f** or **7f**. The M–CO distances are always shorter than the Pt– or Pt′–CO distances.

The spectroscopic characterizations include IR and ^1H, $^{31}P\{^1H\}$, and $^{13}C\{^1H\}$ NMR data. The carbonyl ligands are equivalent on the NMR time scale but not on the IR time scale (ν(CO) between 1750 and 1690 cm^{-1} for the semi triply bridging C(2)O(2) and between ca. 1900 and 1800 cm^{-1} for the semibridging C(1)O(1) and C(3)O(3) ligands).

A bonding description for this family of 58-electron clusters was suggested, considering the 18-electron $[M(CO)_3Cp]^-$ fragments as 4-electron donors toward the L→Pt(I)–Pt(I)←L moiety. This highly unusual bonding mode of the *three*-legged piano-stool $[M(CO)_3Cp]^-$ fragments, capping the *two* Pt atoms (situated within the $M(CO)_3$ cone angle), has only been observed in the corresponding Pd_2M_2 clusters.[1] Provided electronic, steric, and symmetry properties are suitable, more related examples should now become available.[93,94]

Two different strategies have been developed for the synthesis of these Pt_2M_2 clusters. Method A involved the reaction of the sodium carbonylmetalates $Na[M(CO)_3Cp]$ with the $PtCl_2(PR_3)_2$ complexes. This redox reaction occurred with ligand exchange and cluster formation. These observations have been explained in terms of the steric bulk of the PR_3 ligands preventing the formation of the *trans*-$Pt[M(CO)_3Cp]_2(PR_3)_2$ trimetallic complexes, observed and isolated only when the 2-electron donor ligands about the platinum are sterically not demanding.[7,8] In method B, 1 equiv of PR_3 was reacted with the linear trimetallic complexes *trans*-$Pt[M(CO)_3Cp]_2(PhCN)_2$ (M = Cr, Mo, W). These new complexes were isolated and characterized as well as *trans*-$Pt[Cr(CO)_3Cp]_2(t\text{-}BuNC)_2$ (**1b**) and *trans*-$Pt[Cr(CO)_3Cp]_2(c\text{-}C_6H_{11}NC)_2$ (**1c**). The success of method B for preparing heterotetrametallic clusters from heterotrimetallic complexes is based on the phosphine-induced fragmentation of the latter, affording unsaturated fragments that combine with each other in order to form the stable compounds. Method B generally afforded better yields of Pt_2M_2 clusters (up to 87%) than method A. Mechanisms involving radical intermediates are proposed for both methods. None of these methods could be extended to the preparation of mixed Pt–Mn clusters.[36] Instead, they afforded the $Pt_5(CO)_6(PPh_3)_4$ cluster. Of the trimetallic complexes reported, only *trans*-$Pt[Mn(CO)_5]_2(PhCN)_2$ (**4a**) reacted with CO under mild conditions to give *trans*-$Pt[Mn(CO)_5]_2(CO)_2$ (**4d**).

Acknowledgment. We thank Prof. J. Dehand for providing us with technical facilities and for his interest throughout this work. We are grateful to Prof. J. H. Nelson (University of Nevada) for helpful comments on the manuscript. We express our thanks to E. Kremp, Dr. R. Graff, and J. D. Sauer for their assistance in obtaining the NMR spectra. We thank the DGRST for a grant to J.-M.J. and the CNRS for financial support under GRECO-CO.

Registry No. **1a**, 93084-48-1; **1b**, 93084-49-2; **1c**, 93110-17-9; **2a**, 93084-50-5; **3a**, 93084-51-6; **4a**, 93084-52-7; **4d**, 93218-65-6; **5f**, 93110-18-0; **5g**, 93084-53-8; **5h**, 93084-54-9; **6e**, 93084-55-0; **6f**, 71530-81-9; **6g**, 93084-56-1; **6h**, 93084-57-2; **7e**, 93084-58-3; **7f**, 71489-38-8; **7g**, 93084-59-4; **7h**, 71489-37-7; $[Cr(CO)_3Cp]_2$, 12194-12-6; $[Cr(CO)_2Cp]_2$, 54667-87-7; $Pt_5(CO)_6(PEt_3)_4$, 68875-49-0; *trans*-$PtHCl(PEt_3)_2$, 16842-17-4; $[Mo(CO)_3Cp]_2$, 12091-64-4; $Mo_2Cp_2(CO)_5PPh_3$, 12119-01-6; $Pt_5(CO)_6(PPh_3)_4$, 68875-50-3; *trans*-$PtHCl(PPh_3)_2$, 16841-99-9; $[W(CO)_3Cp]_2$, 12091-65-5; $Pt_5(CO)_6(P\text{-}n\text{-}Bu_3)_4$, 93110-19-1; $Mo_2Cp_2(CO)_5(PMe_3)$, 93084-60-7; $[Pt(CO)PPh_3]_n$, 93084-62-9; *trans*-$PtCl_2(PhCN)_2$, 51921-56-3; *trans*-$PtCl_2(t\text{-}BuNC)_2$, 69501-44-6; *trans*-$PtCl_2(c\text{-}C_6H_{11}NC)_2$, 76376-36-8; *trans*-$PtCl_2(PEt_3)_2$, 13965-02-1; *cis*-$PtCl_2(PEt_3)_2$, 15692-07-6; *trans*-$PtCl_2(PPh_3)_2$, 14056-88-3; $Na[Cr(CO)_3Cp]$, 12203-12-2; $Na[Mo(CO)_3Cp]$, 12107-35-6; $Na[W(CO)_3Cp]$, 12107-36-7; $Na[Mn(CO)_5]$, 13859-41-1.

Supplementary Material Available: Quantitative data for the syntheses of **1a–4a** (Table IV) and for cluster syntheses by method A (Table VI) and method B (Table VII), bond lengths (Table XVIS), bond angles (Table XVIIS), selected least-squares planes (Table XVIII), observed and calculated structure factors (Tables XXI–XXIII), and anisotropic thermal parameters for **5f**, **6f** (A and B), and **7f** (A and B) (Tables XXIV–XXVII) (102 pages). Ordering information is given on any current masthead page.

(95) Braunstein, P.; de Méric de Bellefon, C.; Lanfranchi, M.; Tiripicchio, A. *Organometallics* **1984**, *3*, 1772.